Group 1 and group 2 metal complexes supported by a bidentate bulky iminopyrrolyl ligand: synthesis, structural diversity, and ε-caprolactone polymerization study†

Ravi K. Kottalanka, A. Harinath, Supriya Rej and Tarun K. Panda*

We report here a series of alkali and alkaline earth metal complexes, each with a bulky iminopyrrolyl ligand [2-(Ph$_3$CN=CH)C$_4$H$_3$NH] (**1-H**) moiety in their coordination sphere, synthesized using either alkane elimination or silylamine elimination methods or the salt metathesis route. The lithium salt of molecular composition [Li(2-(Ph$_3$CN=CH)C$_4$H$_3$N)(THF)$_2$] (**2**) was prepared using the alkane elimination method, and the silylamine elimination method was used to synthesize the dimeric sodium and tetra-nuclear potassium salts of composition [(2-(Ph$_3$CN=CH)C$_4$H$_3$N)Na(THF)]$_2$ (**3**) and [(2-(Ph$_3$CN=CH)-C$_4$H$_3$N)K(THF)$_{0.5}$]$_4$ (**4**) respectively. The magnesium complex of composition [(THF)$_2$Mg(CH$_2$Ph)-{2-(Ph$_3$CN=CH)C$_4$H$_3$N}] (**5**) was synthesized through the alkane elimination method, in which [Mg(CH$_2$Ph)$_2$(OEt$_2$)$_2$] was treated with the bulky iminopyrrole ligand **1-H** in 1:1 molar ratio, whereas the bis(iminopyrrolyl)magnesium complex [(THF)$_2$Mg{2-(Ph$_3$CN=CH)C$_4$H$_3$N}$_2$] (**6**) was isolated using the salt metathesis route. The heavier alkaline earth metal complexes of the general formula {(THF)$_n$M(2-(Ph$_3$CN=CH)C$_4$H$_3$N)$_2$} [M = Ca (**7**), Sr (**8**), and n = 2; M = Ba (**9**), n = 3] were prepared in pure form using two synthetic methods: in the first method, the bulky iminopyrrole ligand **1-H** was directly treated with the alkaline earth metal precursor [M{N(SiMe$_3$)$_2$}$_2$(THF)$_n$] (where M = Ca, Sr and Ba) in 2:1 molar ratio in THF solvent at ambient temperature. The complexes **7–9** were also obtained using the salt metathesis reaction, which involves the treatment of the potassium salt (**4**) with the corresponding metal diiodides MI$_2$ (M = Ca, Sr and Ba) in 2:1 molar ratio in THF solvent. The molecular structures of all the metal complexes (**1-H**, **2–9**) in the solid state were established through single-crystal X-ray diffraction analysis. The complexes **5–9** were tested as catalysts for the ring-opening polymerization of ε-caprolactone. High activity was observed in the heavier alkaline earth metal complexes **7–9**, with a very narrow poly-dispersity index in comparison to that of magnesium complexes **5** and **6**.

Introduction

Biodegradable polyesters such as poly(ε-caprolactone) (PCL) and poly(lactic acid) (PLA) have attracted widespread interest from industrial and academic research groups, particularly polylactones, which are widely used in medicinal applications such as drug delivery systems, medical sutures, and as plastic modifiers in industries.[1–3] Although they can be obtained by traditional poly-condensation reactions,[4] these polymers are

Department of Chemistry, Indian Institute of Technology Hyderabad, Kandi – 502 285, Sangareddy, Telangana, India. E-mail: tpanda@iith.ac.in;
Fax: +91 (40)2301 6032; Tel: +91 (40)2301 6036
†Electronic supplementary information (ESI) available. CCDC 1418542–1418550. For ESI and crystallographic data in CIF or other electronic format see DOI: 10.1039/c5dt03222a
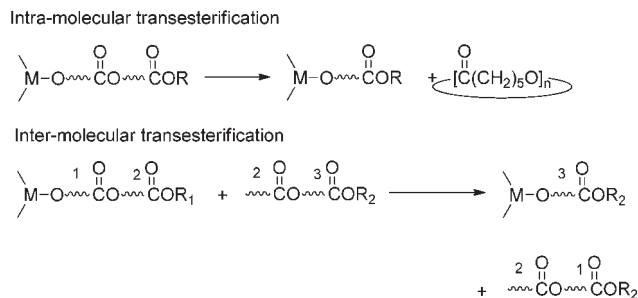
best prepared through the ring-opening polymerization (ROP) of cyclic esters. Macromolecular engineering of these polymers is gaining importance for the synthesis of telechelics, block, graft, and star-shaped polymers.[5] This, in turn, requires the synthesis of polyesters with predictable molecular weights, low polydispersity indices, and control over end groups. Various metal complexes such as aluminium,[6] titanium,[7] tin,[8] zinc,[9] magnesium,[10] and rare earth metals[11] have been used as initiators for the ROP of ε-caprolactone (ε-CL). In many cases, the molecular weight distribution of PCL became broader after the monomer was completely consumed, which suggested the occurrence of trans-esterification (Chart 1).[11b,12] These trans-esterifications occur very often during the polymerization of ε-CL by metal alkoxides, and the rate at which they occur are related to both the nature of the metal ion and the groups surrounding the ion. Subsequently, it was shown that sterically

Intra-molecular transesterification

Inter-molecular transesterification

Chart 1 Intramolecular and intermolecular trans-esterification.

demanding groups attached to a metal ion can prevent PCL chains from coordinating to the ion, and therefore minimize trans-esterification reactions.[13]

Thus, the development of very efficient metal initiators with strong control over the initiation, propagation, and termination steps is needed to synthesize polyesters with predictable molecular weights and narrow polydispersity indices. So far, the ROP process initiated by the heavier alkaline earth (Ae) metals calcium, strontium, and barium has been explored less when compared to other metal complexes,[6–13] and only a few well-defined neutral heteroleptic and homoleptic Ae ROP catalysts are mentioned in the literature.[14,15] This reflects the lack of information in the literature about the synthesis, stability, and reactivity of complexes of these highly electropositive metals. Recurring issues typical of Ca, Sr, and Ba complexes include their kinetic lability with Schlenk-type equilibria in solution.[16] However, significant efforts have been made of late in order to make them friendly and exploit the high reactivity of these complexes. Strategies aimed at suppressing solution distribution equilibria through the careful selection of ancillary ligands such as tris(pyrazolyl)borates,[17] β-diketiminates,[18] aminotrop-(on)iminates,[19,20] or bulky nucleophilic substituents have been invented,[21] while the range of synthetic precursors is growing steadily.[22,23] As a result, single-site Ae-based catalysts have shown an astounding ability for a variety of transformations involving σ-bond metathesis processes.[24]

Recently, iminopyrrole ligands have been commonly employed in the synthesis of several transition metals and rare earth metal compounds.[25] The metal complexes including main group metals, transition metals as well as rare earth metals with 2-iminopyrrolyl in their coordination spheres act as efficient polymerization catalysts.[26] The Mashima group reported a series of alkaline earth metal complexes stabilized by the $[2-(2,6-^iPr_2C_6H_3N{=}CH)C_4H_3NH]$ ligand and those Ae-complexes act as efficient catalysts for the ROP of ε-CL. They also investigated the effects of ionic radii of metal ions on the rate of polymerization and concluded that it was rather good for heavier alkaline earth metal complexes.[27] However, we have noticed that PCLs obtained by heavier alkaline earth metal complexes supported by the $[2-(2,6-^iPr_2C_6H_3N{=}CH)C_4H_3NH]$ ligand have moderate polydispersity indices (PDI = 2.0 for Ba and 1.9 for Mg complexes). This could be due to intra or inter-molecular trans-esterification reactions or other side reactions, which are very common in the ROP of cyclic esters (Chart 1). In our ongoing research into heavier alkaline earth metal chemistry, we have previously reported a series of alkaline earth metal complexes with amidophosphine-chalcogenides/boranes $[R_2NHPh_2P(E)]_n$ (R = $C(CH_3)_3$, $CHPh_2$, CPh_3, $^*CH(CH_3)(Ph)$, $-CH_2-CH_2-$; E = O, S, Se, and BH_3; n = 1 or 2) in their coordination spheres.[28] In these complexes the anionic ligands presented novel molecular structural characteristics via coordination from the amido-nitrogen atom and coordination from the chalcogenide atom or borane group through the hydrogen atoms either in a η^1 or η^2 fashion. A few such complexes have presented excellent catalytic activity towards the ROP of ε-CL.[28d,f]

In this context, we introduce another sterically demanding ancillary ligand $[2-(Ph_3CN{=}CH)-C_4H_3NH]$ (**1-H**) into alkaline earth metal coordination chemistry. We envisage that the sterically demanding bulky substituent on the imine nitrogen atom will completely shield the metal ion, preventing trans-esterification or other side reactions to afford narrower polydispersity indices for PCL (Chart 2).

Here, we describe the detailed synthesis and structural studies of a bidentate rigid bulky-iminopyrrolyl ligand $[2-(Ph_3CN{=}CH)-C_4H_3NH]$ (**1-H**) and its corresponding alkali metal complexes $[Li\{2-(Ph_3CN{=}CH)C_4H_3N\}(THF)_2]$ (**2**), $[\{2-(Ph_3CN{=}CH)-C_4H_3N\}-Na(THF)]_2$ (**3**), and $[\{2-(Ph_3CN{=}CH)-C_4H_3N\}-K(THF)_{0.5}]_4$ (**4**), and alkaline earth metal complexes $[(THF)_2Mg(CH_2Ph)\{2-(Ph_3CN{=}CH)C_4H_3N\}]$ (**5**), $[(THF)_2Mg-\{2-(Ph_3CN{=}CH)C_4H_3N\}_2]$ (**6**), and $[(THF)_nM\{2-(Ph_3CN{=}CH)-C_4H_3N\}_2]$ (M = Ca (**7**), Sr (**8**) and n = 2; M = Ba (**9**), n = 3). We also report in detail the ROP study of ε-CL using newly synthesized alkaline earth metal complexes (**5–9**) as catalysts with different monomer/catalyst ratios.
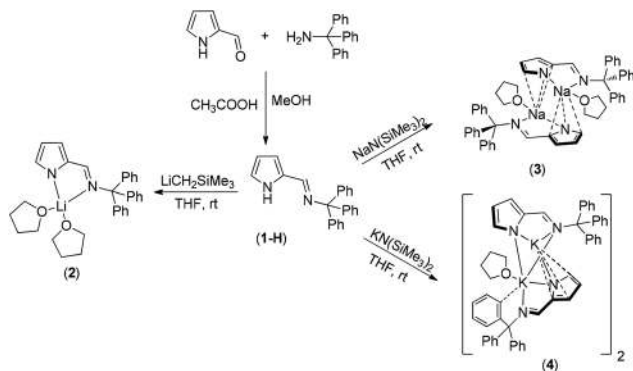
Results and discussion

Ligand synthesis

The (E)-N-((1H-pyrrol-2-yl)methylene)-1,1,1-triphenylmethanamine ligand $[2-(Ph_3CN{=}CH)C_4H_3NH]$ (**1-H**) was prepared in good yield and high purity by the condensation reaction of
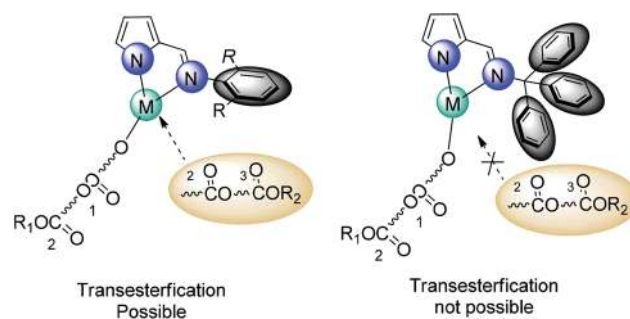
Chart 2 Control of trans-esterification in ROP by changing substituent on imine nitrogen of iminopyrrolyl ligand.

Scheme 1 Synthesis of ligand **1-H** and corresponding alkali metal complexes **2–4**.

Fig. 1 Solid-state structure of ligand **1-H**. All hydrogen atoms (except H1) are omitted for clarity. Selected bond lengths (Å) and bond angles (°): C1–N1 1.357(6), C1–C2 1.364(8), C2–C3 1.410(7), C3–C4 1.372(7), C4–C5 1.433(6), N2–C5 1.260(6), N2–C6 1.485(6), C6–C7 1.544(7), C6–C13 1.552(6), C6–C19 1.530(6); C1–N1–C4 109.3(4), C4–C5–N2 122.6(5), C5–N2–C6 120.6(4), N2–C6–C7 104.2(4).
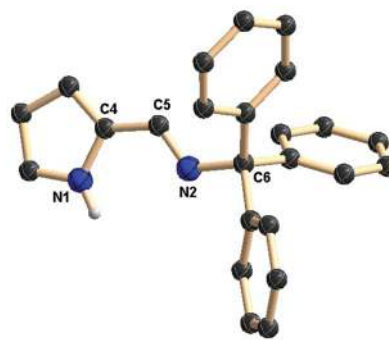
pyrrol-2-carboxyaldehyde with 1 equiv. of tritylamine in the presence of a catalytic amount of glacial acetic acid in methanol solvent (Scheme 1). The ligand **1-H** was fully characterized using standard spectroscopic/analytical techniques and its solid-state structure was established using single-crystal X-ray diffraction analysis.

A strong absorption band observed at 1629 cm^{-1} in FT-IR spectra indicates a C═N bond in the ligand **1-H**. This value is within the range reported in the literature.[29,30] The ^{1}H NMR spectrum of ligand **1-H** showed a broad resonance signal at δ 9.56 ppm for the N–H proton of the pyrrole moiety. The singlet resonance signal at δ 7.71 ppm can be assigned to the imine N═C–H proton. In addition, the singlet at 6.96 ppm, doublet at 6.45 ppm, and multiplets centered at 6.29 ppm in the ^{1}H NMR spectrum clearly represent the resonance of pyrrole ring protons. In the ^{13}C{^{1}H} NMR spectrum, we observed a strong resonance signal at δ 150.2 ppm for the imine carbon atom –C═N, which is in good agreement for the compound [2-(2,6-^{i}Pr$_2$C$_6$H$_3$N═CH)–C$_4$H$_3$NH] (δ 153.2 ppm) and for the compound [2-(2-Ph$_2$PC$_6$H$_4$N═CH)–C$_4$H$_3$NH] (δ 148.7 ppm) reported in the literature.[8] The resonance signal at δ 77.8 ppm corresponds to the tertiary carbon atom of the CPh$_3$ group.

The bulky iminopyrrolyl ligand **1-H** readily crystallizes in CH$_2$Cl$_2$ at room temperature and therefore, the solid-state structure was established using single-crystal X-ray diffraction analysis. The molecular structure of ligand **1-H** is shown in Fig. 1 and details of the structural parameters are given in Table TS1 in the ESI.† Ligand **1-H** crystallizes in the monoclinic space group $P2_1/c$ with two independent molecules in the asymmetric unit. The bond distance of 1.357(6) Å observed for C1–N1 is in good agreement with the value reported for the compound [2-(2,6-^{i}Pr$_2$C$_6$H$_3$N═CH)–C$_4$H$_3$NH][31] [1.354(4) Å] and for the [2-(2,6-^{i}Pr$_2$C$_6$H$_3$N═CMe)–C$_4$H$_3$NH] [1.3604(17) Å].[32] The C5–N2 bond distance was 1.260(6) Å, which is slightly shorter than the C2–N5 distance of 1.2835(19) Å for the compound [2-(2,6-^{i}Pr$_2$C$_6$H$_3$N═CMe)–C$_4$H$_3$NH].[32]

Synthesis and characterization of alkali metal complexes

Treatment of LiCH$_2$SiMe$_3$ with 1 equiv. of the bulky iminopyrrolyl ligand **1-H** in THF solvent resulted in the corresponding

lithium complex of the molecular formula [Li{2-(Ph$_3$CN═CH)-C$_4$H$_3$N}(THF)$_2$] (**2**). Similarly, treatment of 1 equiv. of either sodium or potassium bis(trimethylsilyl)amide with **1-H** in THF solvent resulted in the corresponding dimeric sodium complex [(2-(Ph$_3$CN═CH)C$_4$H$_3$N)Na(THF)]$_2$ (**3**) and tetra-nuclear potassium complex of molecular composition [(2-(Ph$_3$CN═CH)-C$_4$H$_3$N)K(THF)$_{0.5}$]$_4$ (**4**) in very good yield (Scheme 1).[33] The alkali metal complexes **2–4** were fully characterized using standard spectroscopic/analytical techniques and their solid-state structures were established using single-crystal X-ray diffraction analysis. The ^{1}H NMR spectra of compounds **2–4** showed a singlet resonance signal at δ 8.04 (for **2**), 8.03 (for **3**), and 8.17 (for **4**) indicating the presence of the imine proton in each complex. The ^{13}C{^{1}H} NMR spectra also supported the presence of the imine carbon atom in each complex, showing resonance signals at δ 147.9 (for **2**), 147.8 (for **3**), and 147.9 (for **4**). The other pyrrole ring protons and aromatic protons showed resonance signals in each complex at expected regions. Both complexes **3** and **4** displayed only one set of signals in solution, which indicates their dynamic behavior in the solution state. In the solid state, lithium complex **2** crystallized in the orthorhombic space group *Pbca* with 16 molecules in the unit cell. The details of the structural parameters are given in the ESI.† The solid-state structure confirmed the κ^2-NN ligation of ligand **1** with two THF molecules. Complex **2** is shown in Fig. 2. The iminopyrrolyl ligand **1** acts as a bidentate chelating ligand and coordinates to the lithium center through the pyrrolide nitrogen and imine nitrogen atoms. Therefore, the geometry around the lithium ion in **2** can be best described as distorted tetrahedral with bond angles of 87.7(3)° for N1–Li1–N2, 114.0(4)° for O1–Li1–N1, 110.9(3)° for O2–Li1–N1, 115.5(4)° for N2–Li1–O1, 120.5(4)° for N2–Li1–O2, and 107.20(18)° for O1–Li1–O2. The Li–N bond lengths of 1.993(8) and 2.097(7) Å observed in compound **2** are in good agreement with the Li–N bond lengths found in the reported molecules. For example, Li–N bond lengths of 2.068(3) and 2.085(3) Å were observed in the complex {[η^2:η^1-2-(2,6-Me$_2$C$_6$H$_3$N═CH)C$_4$H$_3$N]-

Fig. 2 Solid-state structure of lithium complex 2. All hydrogen atoms (except H10) are omitted for clarity. Selected bond lengths (Å) and bond angles (°): Li1–N1 1.993(8), Li1–N2 2.097(7), Li1–O1 1.944(7), Li–O2 1.946(9), N1–C1 1.345(4), C1–C2 1.397(6), C2–C3 1.401(5), C3–C4 1.408(5), N1–C4 1.366(4), C4–C5 1.431(4), N2–C5 1.289(5), N2–C6 1.492(4), C6–C13 1.550(5); N1–Li–N2 87.7(3), N1–Li1–O1 114.0(4), N1–Li1–O2 110.9(3), N2–Li1–O1 115.5(4), N2–Li1–O2 120.5(4), O1–Li1–O2 107.2(3), C4–C5–N2 122.4(3), N1–C4–C5 121.3(3), N1–C4–C3 111.4(3), N1–C1–C2 112.3(3), Li1–N1–C4 104.6(3), Li1–N2–C5 103.6(3), Li1–N2–C6 138.4(3), N2–C6–C13 107.3(2).
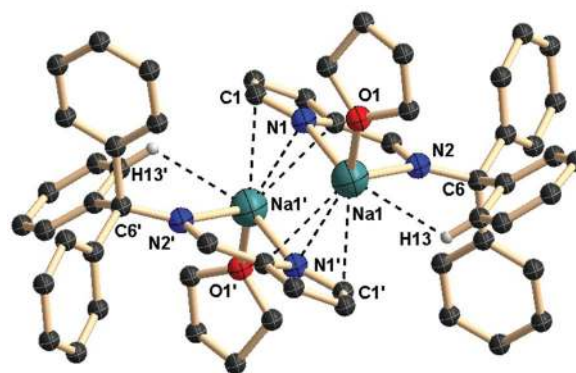
Fig. 3 Solid-state structure of sodium complex (3). All hydrogen atoms (except H13) are omitted for clarity. Selected bond lengths (Å) and bond angles (°): Na1–N1i 2.3586(17), Na1–N2 2.4641(16), Na1–O1 2.3315(17), Na1–N1 2.6998(17), Na1–C1 2.8670(19), Na1–C2 3.080(2), Na1–C3 3.034(2), Na1–C4 2.790(2), Na1–C5 3.0870(19), C4–C5i 1.436(3), C5–N2 1.289(2), N2–C6 1.493(2), C1–N1 1.382(2), C1–C2 1.403(3), C2–C3 1.396(3), C3–C4 1.396(3); N2–Na1–N1i 75.44(5), N1–Na1–N2 95.46(5), N1–Na1–O1 147.46(6), N2–Na1–O1 117.06(6), N1i–Na1–O1 102.83(6), N1–Na1–N1i 85.56(6), C1–Na1–O1 144.32(7), C2–Na1–O1 117.02(6), C3–Na1–O1 105.33(6), C4–Na1–O1 118.92(6).

Li(THF)}$_2$ and 2.105(4) and 2.088(4) Å were observed in the lithium complex {[η^2:η^1-2-(2,6-^{i}Pr$_2$C$_6$H$_3$N=CH)C$_4$H$_3$N]Li(THF)}$_2$.[34] The C1–N1 bond distance of 1.345(4) Å and C5–N2 bond distance of 1.289(5) Å of the anionic ligand moiety are in the range similar to that of the free ligand 1-H [1.357(6) Å for C1–N1 and 1.260(6) Å for C5–N2] upon coordination to the lithium ion. The Li–O bond distances of 1.944(7) and 1.946(9) Å are within the range of Li–O bond distances reported in the literature. Therefore, in the lithium complex 2 a five-membered metallacycle Li1–N1–C4–C5–N2 was formed with a bite angle of 87.7(3)°.

The sodium complex 3 crystallizes in the monoclinic space group $P2_1/n$, with two molecules in the unit cell. The details of the structural parameters are given in TS1 in the ESI.† The solid-state structure of complex 3 confirms its dimeric structure owing to the larger size of the sodium ion than the lithium ion when compared to the monomeric lithium complex 2. The solid-state structure and selected bond lengths and bond angles are shown in Fig. 3. In the dimeric sodium complex 3, each sodium ion is surrounded by one anionic ligand moiety in a bidentate (κ^2) fashion and one THF molecule. Each sodium ion further has π-interactions with pyrrole ring carbons in η^3 mode in the dimeric sodium complex 3. Therefore, each ligand in the dimeric sodium complex 3 bonds to the sodium ions in (σ + π) mode. The geometry of each sodium ion is best described as distorted tetrahedral, formed due to the coordination between two nitrogen atoms of the iminopyrrolyl ligand, one oxygen atom of the THF molecule, and η^3-coordination from the pyrrolyl ring of the dimer fragment. The bite angles of 95.46(5)° for N1–Na1–N2, 75.44(5)° for N1^i–Na1–N2, and 85.56(6)° for N1–Na1–N1^i were observed for each of the iminopyrrolyls chelated to the sodium atoms. The Na–N bond distances of 2.3586(17) and 2.4641(16)

Å were in the range similar to the Na–N distances observed in the compound [μ^2:κ^2-2-(2,6-Me$_2$C$_6$H$_3$N=CH)C$_4$H$_3$NNa(OEt$_2$)]$_2$ [2.405(3) and 2.4285(3) Å].[31] The distance between the sodium ion and the pyrrole ring atoms (C1, N1, and C4 or C1^i, N1^i, and C4^i) were found to be 2.790(2), 2.6998(17), and 2.8670(19) Å respectively. These distances are somewhat longer when compared to the Na-pyrrolyl centroid distances of 2.447(3) Å and 2.494(3) Å found in the polymeric sodium compounds of the type [{Na(μ^2:κ^2-N,N'-iminopyrrolyl)}$_{2n}$(OEt$_2$)$_{2x}$] ($n ≥ 1$; $x = 0$ or 1), (aryl = C$_6$H$_5$ or 2,6-Me$_2$C$_6$H$_3$),[31] indicating that moderate π-interactions exist between the sodium ions and pyrrolyl rings in the dimeric sodium complex 3. The bond distances of 1.349(2), 1.436(3), and 1.289(2) Å for C1–N1, C4–C5, and C5–N2 respectively were almost unchanged compared to that of the free ligand [C1–N1: 1.357(6), C4–C5: 1.433(6), and C5–N2: 1.260(6) Å] upon coordination to the sodium ion. Therefore, each bidentate iminopyrrolyl ligand forms a five-membered metallacycle Na1–N1–C4–C5–N2 or Na1^i–N1^i–C4^i–C5^i–N2^i with the sodium ion, where the sodium ions are slightly deviated from the planarity. Each sodium ion in the dimeric complex 3 is further stabilized by the coordination from one THF molecule. The Na–O bond distance of 2.3315(17) Å fits well with reports in the literature. A short contact Na⋯H between the sodium ion and one of the phenyl protons (Na1⋯H13 2.707 Å) is observed, which can be characterized as a remote or secondary M⋯H interaction.[35] However, in solution all phenyl protons appear equivalent, as observed in the ^{1}H NMR study, presumably due to the dynamic behavior of the complex.

In contrast to sodium complex 3, the potassium complex 4 crystallizes in the monoclinic space group $P2_1/c$ with two molecules in the unit cell. The solid-state structure and selected
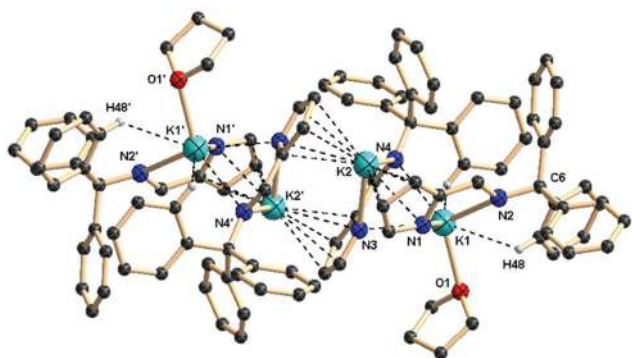
Fig. 4 Solid-state structure of potassium complex **4**. All hydrogen atoms (except H24 and H48) are omitted for clarity. Selected bond lengths (Å) and bond angles (°): K1–N1 2.971(3), K1–N2 3.005(3), K1–N3 2.667(3), K1–N4 3.013(3), K1–O1 2.668(3), K1–C5 3.419(4), K2–N1 3.155(3), K2–N2 2.946(3), K2–N3 3.041(3), K2–C1 3.082(4), K2–C2 3.063(4), K2–C3 3.095(4), K2–C4 3.128(4), C1–N1 1.355(5), C4–N1 1.396(4), C5–N2 1.292(4), C6–N2 1.488(5), C25–N3 1.364(5), C28–N3 1.384(4), C29–N4 1.282(4), C30–N4 1.487(5); N3–K1–O1 114.95(9), N3–K1–N1i 77.85(9), O1–K1–N1i 97.13(9), N3–K1–N2 104.62(8), O1–K1–N2 127.32(8), N1i–K1–N2 58.07(8), N3–K1–N4 60.28(9), O1–K1–N4 112.87(8), N1i–K1–N4 135.55(8), N2–K1–N4 116.53(8), N2–K1–C48 133.36(9), N4–K1–C48 50.33(9), N1i–K2–N2 60.09(8), N1i–K2–N3 74.12(8), N2–K2–N3 97.26(8), N1i–K2–N1 92.85(8), N2–K2–N1 102.47(8), N3–K2–N1 146.71(9).

bond lengths and bond angles are shown in Fig. 4. The asymmetric unit of potassium complex **4** contains two imino-pyrrolyls, two potassium ions, and one coordinated THF molecule. It must be noted that the coordination spheres of both the potassium ions are different. The ion K1 is chelated by two iminopyrrolyl ligands in a bidentate fashion, and one THF molecule, whereas the second ion, K2, is chelated by two nitro-gens from a iminopyrrolyl ligand in a κ^2 fashion and π inter-action (η^5-mode) from one pyrrole ring of the adjacent iminopyrrolyl ligand. Therefore, in the grown structure, two potassium ions (K2 and K2i) are observed as sandwiched between two pyrrolyl ring π-electron densities in a η^5-fashion and further chelated by imine-nitrogen atoms of the imino-pyrrolyls. The other two potassium atoms (K1 and K1i) are sur-rounded by iminopyrrolyl moieties in a bidentate fashion and one THF molecule. Further, K1 has weak interactions with the aromatic ring hydrogen atoms (K1···H24 and K1···H48). There-fore, the geometry of K1 is best described as distorted trigonal-bipyramidal, while that of K2 as distorted tetrahedral. The K2–N1$_{pyrrolyl}$ and K2–N3$_{pyrrolyl}$ bond distances, 3.155(3) and 3.041(3) Å respectively, fit well with the K–N distances observed in $[K(THF)_2\{Ph_2P(Se)N(CMe_3)\}]_n$ (3.047(3) Å).[28e] The K1–N1$_{pyrrolyl}$ and K1–N3$_{pyrrolyl}$ bond distances of 2.971(3) and 2.667(3) Å respectively, which are in good agreement with K–N distances, were observed in the complexes $[\{Ph_2P(Se)NCHPh_2\}K(THF)_2]_2$ [(2.725(3) Å] and $[\{Ph_2P(BH_3)NCHPh_2\}K(THF)_2]_2$ [(2.691(2) Å] previously reported by our group.[28] The K2–N2$_{imine}$ and K1–N4$_{imine}$ bond distances of 2.946(3) and 3.013(3) Å respect-ively were also observed. An average distance of 2.913 Å for the

potassium-pyrrolyl ring centroid was observed in the potas-sium complex **4**, which indicates that highly electropositive and larger potassium atoms have considerable interactions with pyrrolyl π-electron density. In addition, K1 has very weak interactions with the aromatic ring hydrogen atoms (K1···H24 3.047 Å and K1···H48 2.891 Å), reducing their coordination unsaturation. The observed K1–O1 bond distance is 2.668(3) Å, which is in a range similar to that reported in the literature. To the best of our knowledge this is the only example observed of a μ^2-(η^1-η^5) – binding mode between a pyrrole ring and potas-sium atoms when considering different binding modes such as μ^2-(η^1-η^n)-reported many times in the literature.[36]

Synthesis and characterization of alkaline earth metal complexes

We have synthesized various alkaline earth metal complexes of the bulky iminopyrrolyl ligand using alkane elimination, silyl-amine elimination methods, and salt metathesis routes. The heteroleptic magnesium complex of composition $[(THF)_2Mg-(CH_2Ph)\{2-(Ph_3CN=CH)C_4H_3N\}]$ (**5**) was synthesized through the alkane elimination method, in which $[Mg(CH_2Ph)_2(OEt_2)_2]$ was treated with the bulky iminopyrrole ligand **1-H** in 1 : 1 molar ratio in toluene at ambient temperature (Scheme 2). Re-crystallization from a THF/n-pentane mixture afforded the magnesium complex **5** in good yield. However, the homoleptic bis(iminopyrrolyl)magnesium complex of composition $[(THF)_2-Mg\{2-(Ph_3CN=CH)C_4H_3N\}_2]$ (**6**) was synthesized in 90% yield through the salt metathesis route, where the potassium complex **4** was charged with anhydrous MgI$_2$ in 2 : 1 molar ratio in THF solvent (Scheme 2).

The two magnesium complexes **5** and **6** were fully character-ized using spectroscopic and analytical techniques. The mole-cular structures of complexes **5** and **6** were established by single-crystal X-ray diffraction analysis. In the ^{1}H NMR spectra of **5** and **6** recorded in C$_6$D$_6$, the resonance of the imine proton was observed as a singlet at δ 7.91 ppm (**5**) and 7.66 ppm (**6**). The resonances of the two benzyl protons of the –CH$_2$Ph group were obtained as singlets at δ 1.73 ppm
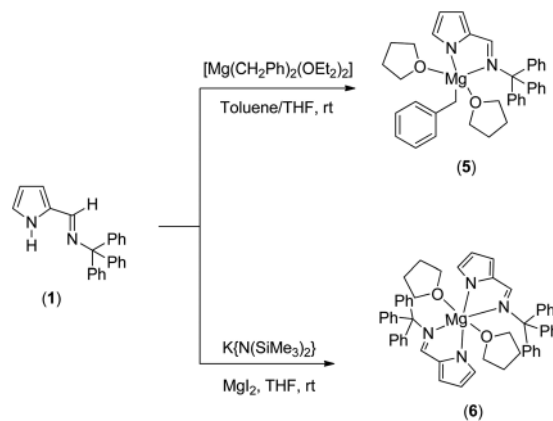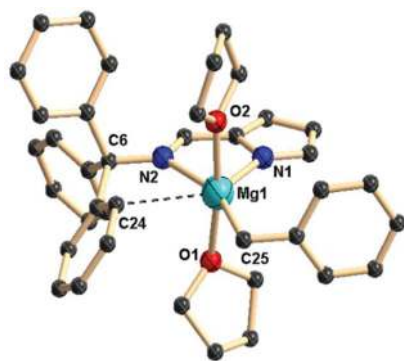

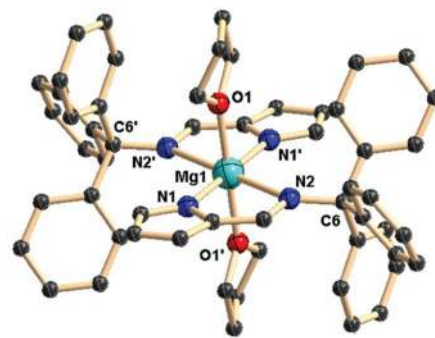**Scheme 2** Synthesis of heteroleptic (**5**) and homoleptic (**6**) magnesium complexes.

for complex **5**. In the $^{13}C\{^1H\}$ NMR spectra, resonance at δ 146.3 ppm (for **5**) and 145.8 ppm (for **6**) can be assigned to the imine carbon (H*C*=N) present in the ligand moiety. However, these values are significantly up-field shifted compared to the free ligand **1-H** (150.3 ppm). In addition, a resonance signal at δ 39.3 ppm was observed for the benzylic carbon atom in complex **5**.

In the solid state, complexes **5** and **6** crystallize in the triclinic space group $P\bar{1}$, with four molecules of **5** and one molecule of **6** in the unit cell. The details of the structural parameters are given in TS1 in the ESI.† The solid-state structures of complexes **5** and **6** confirmed the attachment of one (for **5**) and two (for **6**) iminopyrrolyl ligands to the magnesium ion through the κ^2-NN mode. Fig. 5 and 6 show the molecular structures of complexes **5** and **6** respectively. The central magnesium ion in complex **5** is chelated *via* two nitrogen atoms of the iminopyrrolyl moiety, one benzyl carbon of the –CH$_2$Ph group, and two oxygen atoms from two THF molecules. Thus, the geometry of the magnesium ion in this complex can be best described as distorted trigonal bipyramidal, with two oxygen atoms in the apical position, and two nitrogen atoms and one carbon atom in the basal plane. In contrast, the central magnesium atom in complex **6** is coordinated by two iminopyrrolyl moieties and two THF molecules to adopt a distorted octahedral geometry around the magnesium ion. Both complexes **5** and **6** display two sets of Mg–N distances: one short and one long. The short bond distances Mg–N$_{pyr}$, 2.070(2) (for **5**) and 2.0813(14) Å (for **6**), indicate the Mg–N covalent bond. Mg–N$_{pyr}$ bond distances observed in complexes **5** and **6** are in agreement with reported values; for example, the

Fig. 6 Solid-state structure of homoleptic magnesium complex **6**. Hydrogen atoms are omitted for clarity. Selected bond lengths (Å) and bond angles (°): Mg1–N1 2.0813(14), Mg1–N2 2.5422(14), Mg1–O1 2.1517(12), C1–N1 1.343(2), N1–C4 1.383(2), C4–C5 1.428(2), C5–N2 1.295(2), N2–C6 1.5030(19); N1–Mg1–N1^i 180.0, N2–Mg1–N2^i 180.0, O1–Mg1–O1^i 180.0, N1–Mg1–O1 89.87(5), N2–Mg1–O1 90.80(4), N1–Mg1–N2 75.72(5), N1–Mg1–N2^i 104.28(5), C1–N1–C4 104.92(13), N1–C4–C5 121.60(14), C4–C5–N2 122.89(15), C5–N2–Mg1 103.64(10).

Mg–N bond distance reported as 1.970(3) Å for $[\{(L^{iPr})_2Mg(THF)_2\}\cdot(THF)]$, 2.094(3) Å for $[\{(L^{iPr})_2Mg\}\cdot(THF)]$ (where $L^{iPr} = [(2,6-^iPr_2C_6H_3)NC(Me)]_2)$, and 2.051(2) Å for $[(L^{Mes})_2Mg(THF)_3]$ and 2.070(2) Å for $[(L^{Mes})_2Mg]$ (where $L^{Mes} = [(2,4,6\ Me_3C_6H_2)-NC(Me)]_2).$[37] Recently, our group also synthesized magnesium complexes of the type $[Mg\{C_2H_4(NPh_2P(Se))_2\}\cdot(THF)_3]$ in which we observed Mg–N distances of 2.066(3) and 2.083(3) Å, which are in good agreement with the observed values of 2.070(2) and 2.0813(14) Å for the complexes **5** and **6** respectively.[28e]

The slightly elongated Mg1–N2 distance of 2.200(2) Å in complex **5** represents the coordination bond between the imine nitrogen and the magnesium ion. The Mg–N bond distances also agree well with the Mg–N$_{imine}$ bond distances [2.194(16) Å for $[\{C_4H_3N(2-CH_2NMe_2)\}Mg\{N(SiMe_3)_2\}]_2$; 2.225(10) Å for $[\{C_4H_3N(2-CH_2NEt_2)\}Mg\{N(SiMe_3)_2\}]_2$ reported by Ting-Yu Lee *et al.*[38] In contrast, the Mg–N$_{imine}$ bond length of 2.5422(14) Å in complex **6** is longer than the Mg–N$_{imine}$ distance of 2.200(2) Å observed in complex **5** and literature reports.[28e,37–39] The elongated Mg–N$_{imine}$ bond length in complex **6** can be explained by the steric congestion–created moiety around the magnesium ion by the presence of two bulky triphenyl groups attached to the imine nitrogen atoms of the bulky iminopyrrolyl. In complex **5**, the coordinating nitrogen atoms N1 and N2 formed a bite angle of N1–Mg1–N2 80.98(8)° with the magnesium ion. However, the bite angle of N1–Mg1–N2 75.72(5)° is slightly reduced in complex **6**. In complex **5**, the Mg1–C25 bond distance of 2.185(3) Å is in good agreement with the Mg–C bond distances of 2.1697(17) Å in $[(tmeda)Mg(CH_2Ph)_2]$ and 2.1325(18) Å in $[\eta^2-HC\{C(CH_3)-NAr'\}_2Mg(CH_2Ph)(thf)]$ (Ar' = 2,6-diisopropylphenyl) observed and reported by P. J. Bailey *et al.*[40] In complexes **5** and **6**, the Mg–O bond distances of 2.204 and 2.225 Å (for **5**) and 2.1517(12) Å (for **6**) fit well with the values we previously reported.[28e,38,39] For complex **5**, a five-membered magnesium metallacycle N1–C4–C5–N2–Mg1 and for complex **6**, two five-

Fig. 5 Solid-state structure of heteroleptic magnesium complex **5**. Hydrogen atoms are omitted for clarity. Selected bond lengths (Å) and bond angles (°): molecule 1: Mg1–N1 2.070(2), Mg1–N2 2.200(2), Mg1–C25 2.185(3), Mg1–O1 2.2040(19), Mg1–O2 2.225(2), C1–N1 1.353(3), C1–C2 1.392(4), C2–C3 1.399(3), C3–C4 1.399(3), C4–C5 1.426(3), C4–N1 1.385(3), C5–N2 1.303(3), N2–C6 1.494(3), C6–C7 1.541(3), C25–C26 1.464(4); N1–Mg1–N2 80.98(8), O1–Mg1–O2 173.46(7), N1–Mg1–O1 89.79(8), N1–Mg1–O2 92.71(8), N2–Mg1–O1 84.74(7), N2–Mg1–O2 89.68(7), N1–Mg1–C25 123.72(10), O1–Mg1–C25 92.51(10), O2–Mg1–C25 91.13(10), N2–Mg1–C25 155.19(10), C1–N1–C4 105.8(2), N1–C4–C5 119.0(2), C4–C5–N2 121.2(2), C5–N2–C6 120.02(19), C4–N1–Mg1 110.34(15), C5–N2–Mg1 108.06(15).

membered metallacycles, N1–C4–C5––N2–Mg1 and N1^i–C4^i–C5^i–N2^i–Mg1, are observed due to the κ^2-NN coordination of the iminopyrrolyl ligand **1**.

The heavier alkaline earth metal complexes of composition [M(2-(Ph$_3$CN=CH)C$_4$H$_3$N)$_2$(THF)$_n$] [M = Ca (**7**), Sr (**8**), and n = 2; M = Ba (**9**), n = 3] were synthesized using two methods. In the first method, the bulky iminopyrrolyl ligand **1-H** was directly charged with the corresponding alkaline earth metal bis(trimethylsilyl)amides [M{N(SiMe$_3$)$_2$}$_2$(THF)$_n$] (where M = Ca, Sr, and Ba) in 2 : 1 molar ratio in THF solvent at ambient temperature. The same alkaline earth metal complexes **7–9** were also obtained using the salt metathesis reaction involving the treatment of potassium salt **4** with the corresponding alkaline earth metal diiodides MI$_2$ (M = Ca, Sr and Ba) in 2 : 1 molar ratio in THF solvent (Scheme 3).[33]

In the ^{1}H NMR spectra, each of the complexes **7–9** shows a sharp singlet resonance at δ 7.95 (for **7**), 8.04 (for **8**), and 7.89 (for **9**) ppm, indicating the presence of the imine –C–H proton in the metal complexes, which is slightly downfield shifted compared to the free ligand (7.67 ppm). The coordinated THF molecules can be easily recognized by the ^{1}H NMR spectra as two multiplets centered at 3.61 and 1.76 ppm (for **7**), 3.38 and 1.17 ppm (for **8**), and 3.56 and 1.40 ppm (for **9**). One set of resonance signals was observed for the aromatic ring protons in each metal complex, indicating dynamic behavior in the solution state. The solid-state structures of complexes **7–9** were established through single-crystal X-ray diffraction analysis. The centro-symmetric calcium complex **7** crystallizes in the monoclinic space group $P2_1/n$, with two molecules in the unit cell. In contrast, both the strontium and barium complexes **8** and **9** crystallize in the non-centro-symmetric triclinic space group $P\bar{1}$, with two molecules each in their respective unit cells. The details of the structural parameters are given in TS1 in the ESI.† The molecular structures of complexes **7–9** are shown in Fig. 7a–c respectively. The selected bond lengths and bond angles of complexes **7–9** are given in Table 1. The calcium complex **7** is iso-structural to the corresponding magnesium complex **6**, in which the central calcium ion is surrounded by two anionic iminopyrrolyl ligands and two THF molecules *trans* to each other. Each ligand moiety coordinates to the metal center through the N$_{pyrrolyl}$ and N$_{imine}$ atoms, and forms two five-membered metallacycles, N1–C4–C5–N2–Ca1 and N1i–C4i–C5i–N2i–Ca1, with a bite angle of 71.76(13)°. In complex **8**, the strontium ion was ligated by two chelating
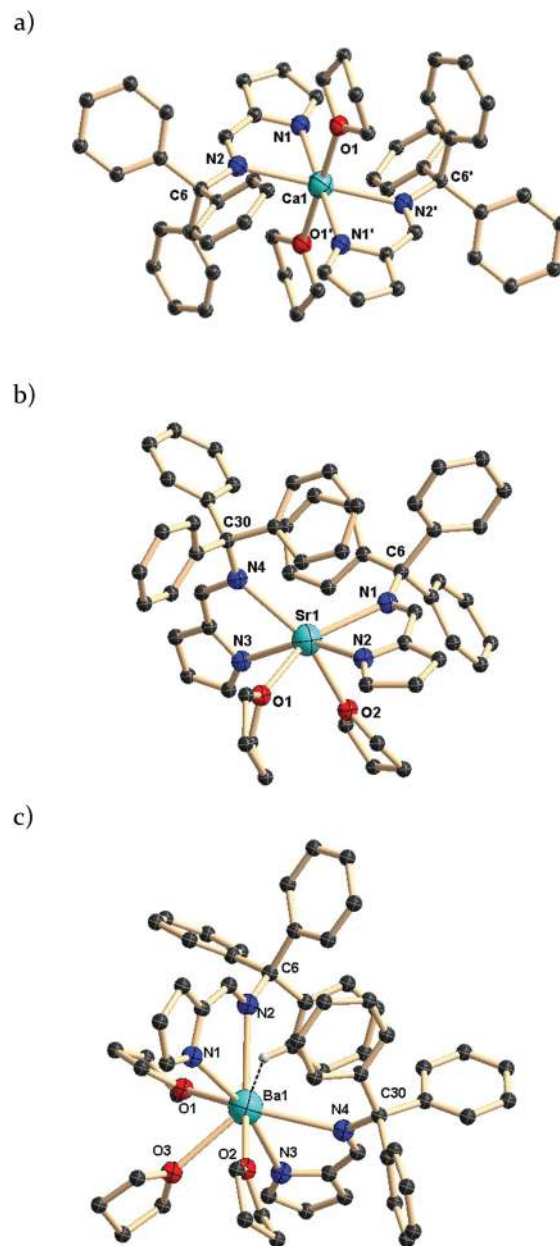
Fig. 7 Solid-state structures of complexes **7** (a), **8** (b), and **9** (c). All hydrogen atoms are omitted for clarity.

bulky iminopyrrolyls and two THF molecules. However, the two THF molecules are *cis* to each other. In both complexes **7** and **8**, the geometry around the central metal ion can be best described as distorted octahedral.

In complex **7**, the Ca–N$_{pyr}$ bond distance of 2.423(4) Å and Ca–N$_{imin}$ bond distance of 2.567(4) Å are in good agreement with the Ca–N bond distances reported for the complexes of composition [(Imp^{Dipp})$_2$Ca(THF)$_2$] [Ca–N1 2.422(2) Å; Ca–N3 2.393(2) Å and Ca–N2 2.526(2) Å; Ca–N4 2.534(2) Å] and [(Imp^{Dipp})Ca(N(SiMe$_3$)$_2$)(THF)$_2$] [Ca–N1 2.388(2) Å; Ca–N3 2.312(2) Å, Ca–N2 2.467(2) Å], and [(Imp^{Me})$_2$Ca(THF)$_2$] [Ca–N1 2.398(4) Å; Ca–N2 2.448(3) Å] (where Imp^{Dipp} = 2-(2,6-C$_6$H$_3^i$Pr$_2$CN=CH)C$_4$H$_3$N
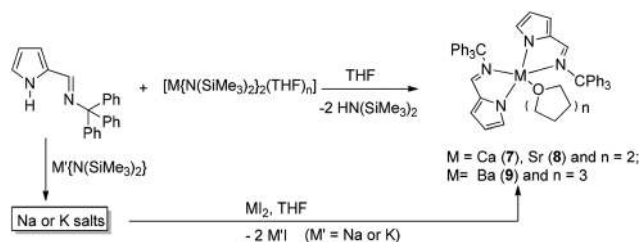
Scheme 3 Synthesis of heavier alkaline earth metal complexes **7–9**.

Table 1 Selected bond lengths (Å) and bond angles (°) of complexes 7–9

	Ca (7)	Sr (8)	Ba (9)
Bond lengths (Å)			
M–N1$_{pyrrolyl}$	2.423(4)	2.570(5)	2.731(5)
		2.546(6)	2.762(5)
M–N2$_{imine}$	2.567(4)	2.677(5)	2.946(5)
		2.679(5)	2.933(5)
M–O1	2.361(4)	2.621(5)	2.812(5)
M–O2	2.361(4)	2.593(5)	2.842(4)
M–O3	—	—	2.830(4)
C4–N1$_{pyrrolyl}$	1.400(5)	1.382(8)	1.348(8)
C5–N2$_{imine}$		1.291(8)	1.304(7)
Bond angles (°)			
N1–M–N2	71.76(13)	68.35(15)	63.78(14)
		68.32(16)	63.14(15)
N1–M–N3	—	154.21(18)	166.32(15)
N1–M–N4	—	129.28(16)	127.40(15)
O1–M–O2	180.00(12)	89.05(17)	134.20(14)
			65.90(14)
			68.76(15)
O1–M–N1	86.72(14)	84.62(17)	89.67(16)
		80.22(17)	84.29(16)
O1–M–N2	89.32(15)	78.967(7)	75.024(5)

and Imp^{Me} = 2-(2,6-C$_6$H$_3$Me$_2$-CN=CH)C$_4$H$_3$N).[27] The Ca1–O1 bond distance of 2.361(4) Å is in the range of normal Ca–O bonds.[41] In complex 8, the Sr–N$_{pyr}$ bond distances of Sr1–N1 2.570(5) Å and Sr1–N3 2.546(6) Å are relatively longer than the corresponding value [2.423(4) Å] observed for complex 7 due to the larger ion radius of strontium when compared to calcium. The Sr–N$_{imine}$ bond distances [Sr1–N2 2.677(5) Å and Sr1–N4 2.679(5) Å] are also longer than the value [2.567(4) Å] observed in complex 7. However, these values are in good agreement with the strontium–nitrogen bond distances [2.6512(2) and 2.669(2) Å] reported previously for the strontium complex [(Imp^{Dipp})$_2$Sr(THF)$_3$] (Imp^{Dipp} = (2,6-^{i}Pr$_2$C$_6$H$_3$N=CH)–C$_4$H$_3$N).[27] In the strontium complex 8, each monoanionic bidentate chelate ligand forms a five-membered metallacycle with the strontium atom N1–C4–C5–N2–Sr1 with a bite angle of 68.35(15)° and N3–C28–C29–N4–Sr1 with a bite angle of 68.32(16)°. The two planes containing the N1, N2, Sr1 and N3, N4, Sr1 atoms are almost orthogonal to each other with a dihedral angle of 85.02°. The Sr–O bond distances, Sr1–O1 2.621(5) Å and Sr1–O2 2.593(5) Å, are in the range of normal Sr–O bonds.[41]

In the barium complex 9, the Ba–N$_{pyr}$ bond distances [Ba1–N1 2.731(5) Å; Ba1–N3 2.762(5) Å] are the longest among all the complexes 7–9 due to the largest ionic radius of Ba^{2+} among three metal ions. However, these values fit well to the Ba–N bond distances reported for the complexes of composition [Ba((Dipp)$_2$DAD)(μ-I)(THF)$_2$]$_2$ [2.720(4) and 2.706(4) Å].[21] The Ba–N$_{imine}$ bond distances of Ba1–N2 2.946(5) Å and Ba1–N4 2.933(5) Å are slightly longer than the Ba–N distances reported for the complexes of composition [(Imp^{Dipp})$_2$Ba(THF)$_2$] [Ba–N1 2.821(5) Å and (Ba–N2 2.823(4) Å] and [Ba((Dipp)$_2$DAD)-(μ-I)(THF)$_2$]$_2$ (2.720(4) and 2.706(4) Å] (where Imp^{Dipp} =

2-(2,6-C$_6$H$_3$^{i}Pr$_2$–CN=CH)–C$_4$H$_3$N).[27,42] The Ba–N bond distances are also comparable to the barium complexes we reported previously.[28] Each ligand moiety is ligated to the barium ion through the N$_{pyr}$ and N$_{imine}$ atoms to form two five-membered metallacycles N1–C1–C5–N2–Ba1 with a bite angle of 63.78(14)° and N3–C28–C29–N4–Ba1 with a bite angle of 63.14(15)°. A dihedral angle of 87.08° between two planes having N1, N2, and Ba1 and N3, N4, and Ba1 atoms indicates the orthogonal arrangement of two five-membered metallacycles to each other. The Ba–O bond distances of Ba1–O1 2.812(5), Ba1–O2 2.842(4), and Ba1–O3 2.830(4) Å are in the range of normal Ba–O bonds reported in the literature.[41]

ROP studies on ε-CL

A series of alkaline-earth metal complexes supported by a bulky iminopyrrolyl ligand were studied as initiators for the living ROP of ε-CL. The typical ring-opening polymerization process is depicted in Scheme 4. We mostly concentrated on living ROP and not on immortal ROP of ε-CL in order to understand the influence of steric bulk on rate of polymerization and the influence of the nature of the metal centre. In the living ROP of cyclic esters, the metal complex acts an initiator, that is, each metal center produces only one polymer chain. On the other hand, an immortal ROP is performed upon addition of a large excess of a protic agent (typically an alcohol) acting as an exogenous initiator and a chain transfer agent, and the complex acts as a catalyst: if the transfer between growing and dormant macromolecules is fast and reversible, the number of polymer chains generated per metal center is equal to the [transfer agent]$_0$-to-[metal]$_0$. The selected data obtained with alkaline-earth metal complexes (5–9) as initiators for living ROP of ε-CL are shown in Table 2. The catalytic efficiency of newly synthesized heteroleptic and homoleptic magnesium complexes 5 and 6 to promote ROP of ε-CL was first evaluated (Table 2, entries 1–6). Indeed, although some previously reported studies on similar magnesium complexes having less-bulky iminopyrrolyls in their coordination sphere gave poor results under similar polymerization conditions,[27] our preliminary investigations on magnesium complexes 5 and 6 showed that they are active in the ROP of ε-CL at 25 °C in toluene with conversion over 90% within 15 minutes (Table 2, entries 1–6).

The molar mass distribution PDI values obtained from GPC analysis are narrow (PDI < 1.8, for entries 1–6) and controlled molecular weight distribution was observed. We noticed that
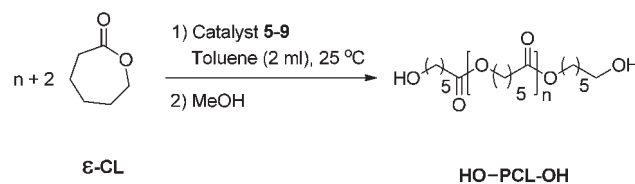

Scheme 4 ROP of ε-CL initiated by alkaline earth metal complexes 5, 7–9.

Table 2 Ring-opening polymerization of ε-caprolactone initiated by alkaline earth metal complexes (5–9)[a]

Entry	Cat. [M]	$[\varepsilon CL]_0/[M]_0$	Reac. time[b] [min]	Conv.[c] [%]	$M_{n(theo)}$[d] [g mol^{-1}]	$M_{n(GPC)}$[e] [g mol^{-1}]	$M_{w(GPC)}$[e] [g mol^{-1}]	M_w/M_n[f]
1	**5**	200/1	10	90	19 826	21 141	31 440	1.48
2	**5**	400/1	10	87	34 847	21 147	31 875	1.50
3	[Mg(CH$_2$SiMe$_3$)(K^2-η^5-bpzcp)][g]	5000/1	10	65	2233	—	151 000	1.45
4	[Mg(CH$_2$SiMe$_3$)(tbpamd)][g]	500/1	1	97	3320	—	52 000	1.41
5	**6**	200/1	15	89	17 824	13 781	21 994	1.59
6	**6**	400/1	15	91	36 449	39 622	72 653	1.83
7	**7**	150/1	5	96	14 419	17 263	26 204	1.51
8	**7**	200/1	5	92	18 425	22 538	37 073	1.64
9	**7**	300/1	10	94	28 238	32 219	50 483	1.56
10	**7**	400/1	10	92	39 613	60 613	97 678	1.61
11	**7**	500/1	15	95	48 065	85 808	138 365	1.61
12	**8**	100/1	5	99	11 896	11 664	12 173	1.04
13	**8**	200/1	5	97	20 397	25 190	34 481	1.36
14	**8**	300/1	5	94	32 944	36 973	55 396	1.49
15	**8**	400/1	10	91	35 087	76 030	93 067	1.22
16	**8**	500/1	10	93	50 288	86 307	137 623	1.59
17	**9**	100/1	5	99	12 887	12 480	13 076	1.04
18	**9**	200/1	5	98	20 608	36 990	46 567	1.25
19	**9**	300/1	5	95	32 343	41 739	55 528	1.33
20	**9**	400/1	10	96	40 374	73 272	105 361	1.43
21	**9**	600/1	10	98	61 824	107 891	139 168	1.28

[a] Results are representative of at least two experiments. [b] Reaction times were not necessarily optimized. [c] Monomer conversions were determined by ^{1}H NMR spectroscopy. [d] Theoretical molar mass values calculated from the relation: [monomer]$_0$/[M]$_0$ × monomer conversion where [M]$_0$ = 8.76 × 10^{-3} mmol and monomer weight of ε-CL = 114 g mol^{-1}. [e] Experimental molar masses were determined by GPC *versus* polyethylene glycol standards. [f] Molar mass distribution was calculated from GPC. [g] These data have been included for comparison in ROP with the alkyl magnesium[43,44] analogues.

the heteroleptic Mg complex (**5**) is more active than the homoleptic Mg complex (**6**). The difference in reactivity could be understood by the initiation steps in both the cases. In the case of complex **5** polymerization follows a nucleophilic route and is initiated by the transfer of an alkyl ligand to the monomer, with cleavage of the acyl–oxygen bond and formation of a metal alkoxide-propagating species.[43] A similar mechanism was also suggested by the A. M. Rodrıguez group for the magnesium complex of composition [Mg(CH$_2$SiMe$_3$)-(κ^2-η^5-bpzcp)] (where bpzcp = 2,2-bis(3,5-dimethylpyrazol-1-yl)-1,1-diphenylethyl cyclopentadienyl) as an initiator for the living ROP of ε-CL.[44] The results obtained therein (PDI < 1.5 with controlled molecular weights) are comparable to our observations (see Table 2) suggesting that the ligand steric bulk and the nature of the metal centre play a crucial role in the ROP of ε-CL. The calcium complex **7** also showed comparable activity towards the ROP of ε-CL with magnesium analogues (**5** and **6**) with narrow PDI values and controlled molecular weight distributions (Table 2, entries 7–11). Indeed, the sluggish reactivity of the calcium complexes is very similar to that observed in some previously reported studies using other calcium complexes for ROP of ε-CL,[45,46] we have noted living polymerization characteristics at room temperature without using any initiating agent like alcohol (entry 9, PDI = 1.5 and M_w = 50 483) indicating that the triphenylmethyl group on the ligand backbone strongly influences the activity of calcium complexes towards the ROP of ε-CL. We anticipated that strontium (**8**) and barium (**9**) complexes could be more active than those of magnesium and calcium complexes

having bulky iminopyrrolyls due to the larger ionic radii of Sr^{2+} and Ba^{2+} ions.[47,48] Both strontium and barium analogues showed higher reactivity towards the conversion of ε-caprolactone to poly-caprolactone and up to 600 ε-CL units were successfully converted in high yields (90 to 98%) within 5–10 minutes at 25 °C. The control over the ROP process was rather good, affording PCLs, with controlled molar mass values, as well as very narrow dispersity data (PDI < 1.4, entries 12–21). Therefore, the overall catalytic efficiency of ring-opening polymerization by heavier alkaline-earth metal complexes (Sr^{2+} and Ba^{2+}) supported by sterically hindered iminopyrrolyl ligands was much better and afforded poly-caprolactone with controlled molecular weights and narrow PDI values. From the ^{1}H NMR spectrum of low-molecular weight PCL by **9** (run 17), we found resonance signals assignable to a terminal iminopyrrolyl group (Fig. S19†), indicating that in the case of amido complexes of alkaline-earth metal complexes (**6–9**) the initial step of the polymerization was a nucleophilic attack of the pyrrolyl nitrogen atom towards the carbonyl carbon of the monomer followed by acyl-oxygen cleavage.

Experimental

General consideration

All manipulations of air-sensitive materials were performed with the rigorous exclusion of oxygen and moisture in flame-dried Schlenk-type glassware either on a dual manifold

Schlenk line, interfaced to a high vacuum (10^{-4} Torr) line, or in an argon-filled M. Braun glove box. THF was pre-dried over Na wire and distilled under nitrogen from sodium and benzophenone ketyl prior to use. Hydrocarbon solvents (toluene and *n*-pentane) were distilled under nitrogen from LiAlH$_4$ and stored in the glove box. ^{1}H NMR (400 MHz) and ^{13}C NMR (100 MHz) spectra were recorded on a Bruker Avance III-400 spectrometer. Bruker Alpha FT-IR was used for FT-IR measurements. Elemental analyses were performed on a Bruker Euro EA at the Indian Institute of Technology Hyderabad and GPC measurements were performed on a Shimadzu LCsolution GPC instrument with polyethylene glycol standards at Graduate School of Engineering Science, Osaka University Japan. Alkaline earth metal diiodides (MgI$_2$, CaI$_2$, SrI$_2$, and BaI$_2$), [NaN(SiMe$_3$)$_2$], [KN(SiMe$_3$)$_2$], pyrrole-2-carboxyaldehyde, tritylamine, and ε-CL were purchased from Sigma Aldrich and used as such. The alkaline earth metal bis(trimethylsilyl)amides [M{N(SiMe$_3$)$_2$}$_2$–(THF)$_n$], (M = Ca, Sr, Ba), [Mg(CH$_2$Ph)$_2$–(OEt$_2$)$_2$] and LiCH$_2$SiMe$_3$ were prepared according to procedures prescribed in the literature.[30,49,50] The NMR solvent C$_6$D$_6$ and CDCl$_3$ were purchased from Sigma Aldrich and dried under either Na/K alloy (for C$_6$D$_6$) or a molecular sieve prior to use.

Preparation of [2-(Ph$_3$CN=CH)C$_4$H$_3$NH] (1-H)

To a dried methanol solution (10 mL) of pyrrole-2-carboxyaldehyde (2.0 g, 21.0 mmol), methanol solution (10 mL) of tritylamine (5.45 g, 21.0 mmol) and a catalytic amount of glacial acetic acid (0.25 mL) were added under stirring. The reaction mixture was stirred for another 12 h at room temperature. The solution was filtered and the solid was washed with cold methanol (5 mL). The compound was dissolved in *n*-hexane (5 mL) and the solvent was evaporated under reduced pressure to afford the final product as an off-white powder. Re-crystallization from hot toluene gave the crystalline product in 79% yield (5.62 g). ^{1}H NMR (400 MHz, CDCl$_3$): δ 9.56 (br, 1H, N-H), 7.71 (s, 1H, N=C–H), 7.35–7.28 (m, 15H, CPh$_3$), 6.96 (d, 1H, 5-pyr), 6.45 (d, 1H, 3-pyr), 6.29 (m, 1H, 4-pyr) ppm. ^{13}C NMR (100 MHz, CDCl$_3$): δ 150.2 (N=CH), 145.9 (ArC), 131.0 (2-pyr), 129.8 (*o*-ArC), 127.7 (*m*-ArC), 126.7 (*p*-ArC), 121.5 (5-pyr), 114.4 (3-pyr), 110.0 (4-pyr), 77.8 (CPh$_3$) ppm. FT-IR (selected frequencies, ν): 3445 (br, N–H), 3025 (w, ArC–H), 1629 (s, C=N) cm^{-1}. Elemental Analysis: C$_{24}$H$_{20}$N$_2$ (336.42): Calcd C 85.68, H 5.99, N 8.33. Found C 85.42, H 5.62, N 8.19.

Preparation of [{2-(Ph$_3$CN=CH)C$_4$H$_3$N}Li(THF)$_2$] (2)

To a THF solution (2 mL) of LiCH$_2$SiMe$_3$ (50 mg, 0.53 mmol), a THF solution (5 mL) of 1 equivalent of ligand **1-H** (178.6 mg, 0.53 mmol) was added dropwise at room temperature under continuous stirring. The mixture was then stirred for 3 h. The solution was kept under reduced pressure to remove the volatile SiMe$_4$ and solvent to give a light yellow product. The yellow residue was washed with *n*-pentane (3 mL) and dried *in vacuo* to afford complex **2** in 85% yield (220.0 mg). Single crystals suitable for X-ray analysis were grown from the THF/*n*-pentane mixture (1 : 2) at −35 °C in one day. ^{1}H NMR (400 MHz, C$_6$D$_6$): δ 8.04 (s, 1H, N=C–H), 7.13–7.11 (m, 9H, CPh3), 7.06 (s, 1H,

5-pyr), 6.98–6.94 (m, 9H, CPh$_3$), 6.43 (d, 1H, 3-pyr), 6.23 (d, 1H, 4-pyr), 3.38–3.36 (m, THF), 1.27–1.23 (m, THF) ppm. ^{13}C{^{1}H} NMR (100 MHz, C$_6$D$_6$): δ 147.9 (N=CH), 130.4 (ArC), 129.4 (2-pyr), 128.3 (*o*-ArC), 128.1 (*m*-ArC), 128.0 (*p*-ArC), 126.6 (5-pyr), 125.7 (3-pyr), 111.6 (4-pyr), 78.5 (CPh3), 67.8 (THF), 25.4 (THF) ppm. FT-IR (selected frequencies, ν): 3025 (w, ArC–H), 1629 (s, C=N) cm^{-1}. Elemental Analysis: C$_{32}$H$_{35}$LiN$_2$O$_2$ (486.29): Calcd C 78.99, H 7.25, N 5.76. Found C 78.64, H 6.98, N 5.56.

Preparation of [{2-(Ph$_3$CN=CH)C$_4$H$_3$N}Na(THF)]$_2$ (3)

To a THF solution (5 mL) of ligand **1-H** (300 mg, 0.89 mmol), a solution of 5 mL THF and one equivalent of sodium bis(trimethylsilyl)amide (163.5 mg, 0.89 mmol) was added dropwise, with stirring, at room temperature. Stirring was continued for another 12 h and the volatile compounds were then removed under reduced pressure. The title compound was obtained as a white solid, which was further purified by washing with *n*-pentane (5 mL). Single crystals suitable for X-ray diffraction analysis were obtained from the THF/*n*-pentane mixture (1 : 2) solvent at −35 °C after one day. 91% Yield (350.0 mg). ^{1}H NMR (400 MHz, C$_6$D$_6$): δ 8.03 (s, 1H, N=C-H), 7.17–7.15 (m, 6H, CPh$_3$), 7.02 (s, 1H, 5-pyr), 6.98–6.91 (m, 9H, CPh$_3$), 6.49 (d, 1H, 3-pyr), 6.27 (d, 1H, 4-pyr), 3.27–3.24 (m, THF), 1.21–1.18 (m, THF) ppm. ^{13}C NMR (100 MHz, C$_6$D$_6$): δ 147.8 (N=CH), 145.9 (ArC), 130.2 (2-pyr), 128.3 (*o*-ArC), 128.1 (*m*-ArC), 127.8 (*p*-ArC), 126.8 (5-pyr), 119.1 (3-pyr), 111.1 (1C, 4-pyr), 78.3 (CPh$_3$), 67.8 (THF), 25.6 (THF) ppm. FT-IR (selected frequencies, ν): 3025 (w, ArC–H), 1629 (s, C=N) cm^{-1}. Elemental Analysis: C$_{56}$H$_{54}$N$_4$Na$_2$O$_2$ (861.01): Calcd C 78.12, H 6.32, N 6.51. Found C 77.94, H 5.99, N 6.38.

Preparation of [{2-(Ph$_3$CN=CH)C$_4$H$_3$N}K(THF)$_{0.5}$]$_4$ (4)

To a THF solution (5 mL) of ligand **1-H** (300 mg, 0.89 mmol), one equivalent of potassium bis(trimethylsilyl)amide (177.8 mg, 0.89 mmol) was added dropwise, with stirring, at room temperature. Stirring was continued for another 12 h and the volatile compounds were then removed under reduced pressure. The title compound was obtained as a white solid, which was further purified by washing with *n*-pentane. Single crystals suitable for X-ray diffraction analysis were obtained from the THF/*n*-pentane mixture (1 : 2) at −35 °C after one day. 95% Yield (380.5 mg). ^{1}H NMR (400 MHz, C$_6$D$_6$): δ 8.17 (s, 1H, N=C–H), 7.18–7.01 (m, 15H, CPh$_3$), 7.11 (s, 1H, 5-pyr), 6.74 (m, 1H, 3-pyr), 6.58 (m, 1H, 4-pyr), 3.22–3.19 (m, THF), 1.22–1.19 (m, THF) ppm. ^{13}C NMR (100 MHz, C$_6$D$_6$): δ 147.9 (N=CH), 137.2 (2-pyr), 130.2 (ArC), 128.8 (*o*-ArC), 128.1 (*m*-ArC), 127.9 (*p*-ArC), 126.8 (5-pyr), 122.4 (3-pyr), 111.3 (4-pyr), 79.2 (CPh3), 68.1 (THF), 25.4 (THF) ppm. FT-IR (selected frequencies, ν): 3026 (w, ArC–H), 1630 (s, C=N) cm^{-1}. Elemental Analysis: C$_{104}$H$_{92}$K$_4$N$_8$O$_2$ (1642.26): Calcd C 76.06, H 5.65, N 6.82. Found C 75.88, H 5.32, N 6.51.

Preparation of [{2-(Ph$_3$CN=CH)C$_4$H$_3$N}–{PhCH$_2$}Mg(THF)$_2$] (5)

In a 25 mL of Schlenk flask one equivalent of ligand **1-H** (100 mg, 0.297 mmol) was dissolved in 10 mL of toluene. To this solution, one equivalent of [Mg(CH$_2$Ph)$_2$(Et$_2$O)$_2$]

(105.4 mg, 0.297 mmol) in toluene (5 mL) was added dropwise at room temperature. The reaction mixture was stirred for 6 h and the solvents were then removed under reduced pressure. The colorless residue was washed with *n*-pentane twice (5 mL) and crystals suitable for X-ray analysis were grown from the THF/*n*-pentane (1 : 2) mixture. Yield 160.5 mg (90%). ^{1}H NMR (400 MHz, C$_6$D$_6$): δ 7.91 (s, 1H, N=C–H), 7.18–7.07 (m, 15H, CPh$_3$), 7.02–6.96 (m, 5H, Ar–H), 6.74 (d, 1H, 5-pyr), 6.66 (m, 1H, 3-pyr), 6.56 (m, 1H, 4-pyr), 1.73 (s, 2H, CH$_2$Ph) ppm. ^{13}C{^{1}H} NMR (100 MHz, C$_6$D$_6$): δ 146.3 (N=CH), 137.8 (ArC), 136.2 (CH$_2$Ph), 135.3 (2-pyr), 129.1 (*o*-CH$_2$Ph), 128.7 (*o*-ArC), 128.1 (*m*-CH$_2$Ph), 127.2 (*m*-ArC), 126.1 (*p*-ArC), 125.4 (*p*-CH$_2$Ph), 127.4 (5-pyr), 121.8 (3-pyr), 114.2 (4-pyr), 77.7 (CPh$_3$), 39.3 (CH$_2$Ph) ppm. FT-IR (selected frequencies, ν): 3025 (w, ArC–H), 1631 (s, C=N) cm^{-1}. Elemental Analysis: C$_{39}$H$_{42}$MgN$_2$O$_2$ (595.06): Calcd C 78.72, H 7.11, N 4.71. Found C 78.39, H 6.93, N 4.46.

Preparation of [{2-(Ph$_3$CN=CH)C$_4$H$_3$N}$_2$Mg(THF)$_2$] (6)

In a pre-dried 25 mL Schlenk flask potassium salt **4** (200 mg, 0.448 mmol) and MgI$_2$ (62.30 mg, 0.224 mmol) were mixed with THF (10 mL) solvent. The reaction mixture was stirred for 12 h at room temperature and a white precipitate of KI was removed by filtration. The solvent was removed under reduced pressure to leave a white residue. The magnesium complex **6** was re-crystallized from the THF/*n*-pentane (1 : 2) mixture. Yield: 175 mg (93%). ^{1}H NMR (400 MHz, C$_6$D$_6$): δ 7.66 (s, 1H, N=C–H), 7.15–7.10 (m, 9H, CPh$_3$), 7.03–6.99 (m, 6H, CPh$_3$), 6.76 (m, 1H, 5-pyr), 6.47 (d, 1H, 3-pyr), 5.85 (m, 1H, 4-pyr), 3.56–3.52 (m, THF), 1.39–1.37 (m, THF) ppm. ^{13}C NMR (100 MHz, C$_6$D$_6$): δ 145.8 (N=CH), 135.6 (2-pyr), 127.9 (ArC), 126.8 (*o*-ArC), 126.0 (*m*-ArC), 124.2 (*p*-ArC), 119.2 (5-pyr), 115.4 (3-pyr), 114.9 (4-pyr), 77.3 (CPh$_3$), 64.5 (THF), 22.4 (THF) ppm. FT-IR (selected frequencies, ν): 3025 (w, ArC–H), 1629 (s, C=N) cm^{-1}. Elemental Analysis: C$_{56}$H$_{54}$MgN$_4$O$_2$ (839.34): Calcd C 80.13, H 6.48, N 6.67. Found C 79.71, H 6.27, N 6.31.

Preparation of [{2-(Ph$_3$CN=CH)C$_4$H$_3$N}$_2$M(THF)$_n$] [M = Ca (7), Sr (8) and n = 2; M = Ba (9) and n = 3]

Route 1: Ligand **1-H** (200 mg, 0.594 mmol) and [Ca{N(SiMe$_3$)$_2$}$_2$(THF)$_2$] (150 mg, 0.297 mmol) were dissolved in THF (5 mL). The reaction mixture was stirred for 6 h at room temperature and all volatiles were removed under reduced pressure. The remaining white solid was washed with *n*-pentane 95 mL) and dried *in vacuo* to give the calcium complex **7** as a white powder. Re-crystallization from THF/*n*-pentane (1 : 2) gave colorless crystals suitable for X-ray diffraction measurements. Yield: 241 mg (95%).

Route 2: In a pre-dried Schlenk flask potassium salt **4** (200 mg, 0.448 mmol) and CaI$_2$ (65.8 mg, 0.224 mmol) were mixed with THF (10 mL) solvent. The reaction mixture was stirred for 12 h at room temperature and the white precipitate of KI was removed by filtration through a G-4 frit. The solvent was evaporated under reduced pressure to give a white residue. The calcium complex **7** was re-crystallized from the THF/*n*-pentane (1 : 2) mixture. Yield: 172 mg (90%). ^{1}H NMR

(400 MHz, C$_6$D$_6$): δ 7.95 (s, 1H, N=C–H), 7.20–7.17 (m, 15H, CPh$_3$), 6.33 (m, 1H, 5-pyr), 6.13 (s, 1H, 3-pyr), 5.89 (m, 1H, 4-pyr), 3.61–3.57 (m, THF), 1.76–1.72 (m, THF) ppm. ^{13}C{^{1}H} NMR (100 MHz, C$_6$D$_6$): δ 157.7 (N=CH), 147.1 (ArC), 136.3(2-pyr), 128.9 (*o*-ArC), 128.2 (*m*-ArC), 125.3 (*p*-pyr), 116.8 (5-pyr), 113.4 (3-pyr), 111.5 (4-pyr), 66.8 (CPh$_3$), 65.4 (THF), 25.1 (THF) ppm. FT-IR (selected frequencies, ν): 3025 (w, ArC–H), 1632 (s, C=N) cm^{-1}. Elemental Analysis: C$_{66}$H$_{70}$CaN$_4$O$_4$ (999.32): Calcd C 77.46, H, 6.89, N 5.47. Found C 76.98, H 6.42, N 5.28.

Other heavier alkaline earth bis(iminopyrrolyl) complexes **8** and **9** were prepared in a manner similar to complex **7** using two routes.

Complex 8

Route 1: Yield 248 mg (92%) and *Route 2*: Yield 182 mg (90%). ^{1}H NMR (400 MHz, C$_6$D$_6$): δ 8.04 (s, 1H, N=C–H), 7.17–6.94 (m, 15H, CPh$_3$), 6.51 (m, 1H, 5-pyr), 6.15 (m, 1H, 3-pyr), 5.92 (m, 1H, 4-pyr), 3.38–3.36 (m, THF), 1.20–1.17 (m, THF) ppm. ^{13}C{^{1}H} NMR (100 MHz, C$_6$D$_6$): δ 163.9 (N=CH), 148.1 (ArC), 137.3 (2-pyr), 130.3 (*o*-ArC), 128.6 (*m*-ArC), 127.8 (*p*-ArC), 122.6 (5-pyr), 116.4 (3-pyr), 111.4 (4-pyr), 79.4 (CPh$_3$), 68.3 (THF), 25.5 (THF) ppm. FT-IR (selected frequencies, ν): 3026 (w, ArC–H), 1629 (s, C=N) cm^{-1}. Elemental Analysis: C$_{60}$H$_{62}$N$_4$O$_3$Sr (974.76): Calcd C 73.93, H 6.41, N 5.75. Found C 73.42, H 6.22, N 5.43.

Complex 9

Route 1: Yield 283 mg (93%) and *Route 2*: Yield 200 mg (88%). ^{1}H NMR (400 MHz, C$_6$D$_6$): δ 7.89 (s, 1H, N=C–H), 7.39–7.37 (m, 6H, CPh$_3$), 7.16–7.03 (m, 9H, CPh$_3$), 6.43 (m, 1H, 5-pyr), 6.25 (s, 1H, 3-pyr), 6.15 (m, 1H, 4-pyr), 3.58–3.55 (m, THF), 1.42–1.39 (m, THF) ppm. ^{13}C{^{1}H} NMR (100 MHz, C$_6$D$_6$): δ 146.8 (N=CH), 130.4 (ArC), 128.3 (*o*-ArC), 128.0 (*m*-ArC), 127.9 (2-pyr), 127.8 (*p*-ArC), 127.0 (5-pyr), 115.4 (3-pyr), 110.2 (4-pyr), 78.3 (CPh$_3$), 67.8 (THF), 25.8 (THF) ppm. FT-IR (selected frequencies, ν): 3025 (w, ArC–H), 1629 (s, C=N) cm^{-1}. Elemental Analysis: C$_{68}$H$_{77}$BaN$_4$O$_5$ (1167.68): Calcd C 69.94, H 6.65, N 4.80. Found C 69.48, H 6.16, N 4.53.

Typical polymerization experiment

In a glove box under an argon atmosphere, the catalyst was dissolved in appropriate amount (1.0 mL) of dry toluene. ε-CL in 1.0 mL of toluene was then added along with vigorous stirring. The reaction mixture was stirred at room temperature for 5–10 minutes, after which the reaction mixture was quenched by addition of a small amount of (1.0 mL) methanol, to which a slight excess of acidified methanol was then added. The polymer was precipitated in excess methanol and it was filtered and dried under vacuum. The final polymer was then analyzed using NMR and GPC.

X-Ray crystallographic studies of complexes 1a, 1d, 2b, 2c, 3a, 4a, 5a

Single crystals of compounds **2–9** were grown from a THF and *n*-pentane mixture at −35 °C under an inert atmosphere.

Single crystals of compound **1-H** suitable for X-ray measurements were obtained from CH_2Cl_2 at room temperature. For compounds **1–9** (except **5** and **7**) a crystal of suitable dimensions was mounted on a CryoLoop (Hampton Research Corp.) with a layer of light mineral oil and placed in a nitrogen stream at 150(2) K and all measurements were made on an Agilent Supernova X-calibur Eos CCD detector with graphite-monochromatic Cu-Kα (1.54184 Å) radiation. For compounds **5** and **7**, data were collected at 113(2) K and measurements were made on a Rigaku RAXIS RAPID imaging plate area detector or a Rigaku Mercury CCD area detector with graphite-monochromated Mo-Kα (0.71075 Å) radiation. Crystal data and structure refinement parameters are summarized in Table TS1 in the ESI.† The structures were solved by direct methods (SIR92)[51] and refined on F^2 by full-matrix least-squares methods; using SHELXL-97.[52] Non-hydrogen atoms were anisotropically refined. H atoms were included in the refinement in calculated positions riding on their carrier atoms. The function minimized was $[\sum w(F_o{}^2 - F_c{}^2)^2]$ (w = $1/[\sigma^2(F_o{}^2) + (aP)^2 + bP]$), where $P = (Max(F_o{}^2,0) + 2F_c{}^2)/3$ with $\sigma^2(F_o{}^2)$ from counting statistics. The functions R_1 and wR_2 were $(\sum||F_o| - |F_c||)/\sum|F_o|$ and $[\sum w(F_o{}^2 - F_c{}^2)^2/\sum(wF_o{}^4)]^{1/2}$ respectively. The Diamond-3 program was used to draw the molecules. Crystallographic data (excluding structural factors) for the structures reported in this paper have been deposited with the Cambridge Crystallographic Data Centre as supplementary publication no. CCDC 1418542–1418550.

Conclusion

We have successfully prepared alkali metal complexes of the bulky iminopyrrolyl ligand and their solid-state structures reveal the flexibility and multidentate behavior of the iminopyrrolyl ligand **1**. In the case of the sodium complex, we observed a dimeric structure whereas, due to lower charge density of the potassium ion, a tetranuclear structure was found in the solid state. The heteroleptic and homoleptic magnesium complexes **5** and **6** respectively were successfully synthesized and characterized using X-ray crystallography. In the solid state, complex **5** is five-fold coordinated and shows a trigonal bipyramidal geometry around the magnesium ion, whereas the magnesium ion in complex **6** adopts a octahedral arrangement due to the six-fold coordination from ligand **1** and THF molecules. The heavier alkaline earth metal complexes **7–9** were synthesized either by silylamine elimination or salt metathesis routes using $[M\{N(SiMe_3)_2\}_2(THF)_n]$ or MI_2 (M = Ca, Sr, and Ba) as starting materials. In the solid state, the effect of the ion radii of the central metal ions as well as the steric bulk of the ligand backbone determined the metal coordination sphere. The calcium complex **7** is centro-symmetric and adopts an octahedral geometry, whereas the strontium and barium complexes (**8** and **9**), due to their larger size, are non-centro-symmetric and adopt distorted octahedral and distorted pentagonal-bipyramidal geometries respectively. In addition, the M–N_{pyr} and M–N_{imine} bonds are relatively longer

than those of the other amido-metal complexes of barium and strontium. The bis(iminopyrrolyl)complexes of strontium (**8**) and barium (**9**) were highly active for the ROP of ε-CL, affording high molecular weight PCLs compared to the polymers produced by the calcium and magnesium complexes.

Notes and references

1 (a) K. E. Uhrich, S. M. Cannizzaro, R. S. Langer and K. M. Shakesheff, *Chem. Rev.*, 1999, **99**, 3181–3198; (b) R. E. Drumright, P. R. Gruber and D. E. Henton, *Adv. Mater.*, 2000, **12**, 1841–1846; (c) A.-C. Albertsson and I. K. Varma, *Biomacromolecules*, 2003, **4**, 1466–1486; (d) S. Mecking, *Angew. Chem., Int. Ed.*, 2004, **43**, 1078–1085; (e) O. Dechy-Cabaret, B. Martin-Vaca and D. Bourissou, *Chem. Rev.*, 2004, **104**, 6147–6176; (f) Y. Sarazin, B. Liu, T. Roisnel, L. Maron and J.-F. Carpentier, *J. Am. Chem. Soc.*, 2011, **133**, 9069–9087.

2 (a) Y. Ikada and H. Tsuji, *Macromol. Rapid Cummun.*, 2000, **21**, 117–132; (b) K. Sudehsh, H. Abe and Y. Doi, *Prog. Polym. Sci.*, 2000, **25**, 1503–1555; (c) M. Vert, *Biomacromolecules*, 2005, **6**, 538–546; (d) L. S. Nair and C. T. Laurencin, *Prog. Polym. Sci.*, 2007, **32**, 762–798.

3 (a) G. Rokicki, *Prog. Polym. Sci.*, 2000, **25**, 259–342; (b) K. M. Stridsberg, M. Ryner and A.-C. Albertsson, *Adv. Polym. Sci.*, 2002, **157**, 42–65; (c) A.-C. Albertsson and I. K. Varma, *Biomacromolecules*, 2002, **3**, 1–41; (d) A. P. Dove, *Chem. Commun.*, 2008, 6446–6470.

4 (a) K. Ito and Y. Yamashita, *Macromolecules*, 1978, **11**, 68–72; (b) N. Spassky, *Makromol. Chem., Macromol. Symp.*, 1991, **42/43**, 15–49; (c) J. Okuda and I. L. Rushkin, *Macromolecules*, 1993, **26**, 5530–5532; (d) A. Duda and S. Penczek, *Macromolecules*, 1995, **28**, 5981–5992; (e) H. R. Kricheldorf and S. Eggerstedt, *Macromolecules*, 1997, **30**, 5693–5697; (f) A. Nakayama, N. A. Nakayama, N. Kawasaki, S. Aiba, Y. Maeda, I. Arvanitoyannis and N. Yamamoto, *Polymer*, 1998, **39**, 1213–1222.

5 (a) T. Ouhadi, A. Hamitou, R. Jerome and P. H. Teyssié, *Macromolecules*, 1976, **9**, 927–931; (b) J. Heuschen, R. Jérôme and P. H. Teyssié, *Macromolecules*, 1981, **14**, 242–246; (c) C. Jacobs, Ph. Dubois, R. Jérôme and P. H. Teyssié, *Macromolecules*, 1991, **24**, 3027–3034; (d) P. Kurcok, P. Dubois, W. Sikorska, Z. Jedlinski and R. Jérôme,

Macromolecules, 1997, **30**, 5591–5595; (*e*) D. Tian, Ph. Dubois and R. Jérôme, *Macromolecules*, 1997, **30**, 1947–1954; (*f*) M. Trollsas, J. L. Hedrick, D. Mecerreyes, Ph. Dubois, R. Jérôme, H. Ihre and A. Hult, *Macromolecules*, 1998, **31**, 2756–2763; (*g*) H. R. Kricheldorf and S. Eggerstedt, *Macromol. Chem. Phys.*, 1998, **199**, 283–290; (*h*) M. Trollsas, B. Atthoff, H. Claesson and J. L. Hedrick, *Macromolecules*, 1998, **31**, 3439–3445; (*i*) H. R. Kricheldorf and K. Hauser, *Macromolecules*, 1998, **31**, 614–620.

6 (*a*) A. Hamitou, T. Ouhadi, R. Jerome and P. H. Teyssié, *J. Polym. Sci.*, 1977, **15**, 865–873; (*b*) M. Endo, T. Aida and S. Inoue, *Macromolecules*, 1987, **20**, 2982–2988; (*c*) R. C. Yu, C. H. Hung, J. H. Huang, H. Y. Lee and J. T. Chen, *Inorg. Chem.*, 2002, **41**, 6450–6455; (*d*) D. Chakraborty and E. Y. X. Chen, *Organometallics*, 2003, **22**, 769–774; (*e*) C. T. Chen, C. A. Huang and B. H. Huang, *Macromolecules*, 2004, **37**, 7968–7973; (*f*) P. Hormnirun, E. L. Marshall, V. C. Gibson, J. P. White and D. J. Williams, *J. Am. Chem. Soc.*, 2004, **126**, 2688–2689; (*g*) N. Nomura, T. Aoyama, R. Ishii and T. Kondo, *Macromolecules*, 2005, **38**, 5363–5366; (*h*) W. Ziemkowska, J. Kochanowski and M. K. Cyrański, *J. Organomet. Chem.*, 2010, **695**, 1205–1209; (*i*) X. Pang, R. Duan, X. Li, Z. Sun, H. Zhang, X. Wang and X. Chen, *RSC Adv.*, 2014, **4**, 57210–57217.

7 (*a*) J. Okuda and I. L. Rushkin, *Macromolecules*, 1993, **26**, 5530–5532; (*b*) Y. Takashima, Y. Nakayama, K. Watanabe, T. Itono, N. Ueyama, A. Nakamura, H. Yasuda and A. Harada, *Macromolecules*, 2002, **35**, 7538–7544; (*c*) A. Arbaoui and C. Redshaw, *Polym. Chem.*, 2010, **1**, 801–826.

8 (*a*) H. Yavuz, C. Babac, K. Tuzlakoglu and E. Piskin, *Polym. Degrad. Stab.*, 2002, **75**, 431–437; (*b*) A. Kowalski, J. Libiszowski, T. Biela, M. Cypryk, A. Duda and S. Penczek, *Macromolecules*, 2005, **38**, 8170–8176; (*c*) G. Jiang, I. A. Jones, C. D. Rudd and G. S. Walker, *J. Appl. Polym. Sci.*, 2009, **114**, 658–662.

9 (*a*) M. Vivas and J. Contreras, *Eur. Polym. J.*, 2003, **39**, 43–47; (*b*) H. Y. Chen, B. H. Huang and C. C. Lin, *Macromolecules*, 2005, **38**, 5400–5405; (*c*) D. J. Darensbourg and O. Karroonnirun, *Macromolecules*, 2010, **43**, 8880–8886.

10 (*a*) E. L. Marshall, V. C. Gibson and H. S. Rzepa, *J. Am. Chem. Soc.*, 2005, **127**, 6048–6051; (*b*) L. F. Hsueh, N. T. Chuang, C. Y. Lee, A. Datta, J. H. Huang and T. Y. Lee, *Eur. J. Inorg. Chem.*, 2011, 5530–5537; (*c*) H. J. Fang, P. S. Lai, J. Y. Chen, S. C. N. Hsu, W. D. Peng, S. W. Ou, Y. C. Lai, Y. J. Chen, H. Chung, Y. Chen, T. C. Huang, B. S. Wu and H. Y. Chen, *J. Polym. Sci.*, 2012, **50**, 2697–2704.

11 (*a*) Y. Shen, *Macromolecules*, 1996, **29**, 3441–3446; (*b*) Y. Shen, Z. Shen, Y. Zhang and K. Yao, *Macromolecules*, 1996, **29**, 8289–8295; (*c*) D. Barbier-Baudry, A. Bouazza, C. H. Brachais, A. Dormond and M. Visseaux, *Macromol. Rapid Commun.*, 2000, **21**, 213–217; (*d*) M. Visseauxa, C. H. Brachaisa, C. Boissonb and T. C. R. Karine, *Acad. Sci. Paris, Série IIc, Chimie 3*, 2000, 631–638; (*e*) Y. Matsuo, K. Mashima and K. Tani, *Organometallics*, 2001, **20**, 3510–

3518; (*f*) L. Zhang, C. Yu and Z. Shen, *Polym. Bull.*, 2003, **51**, 47–53; (*g*) K. Nakano, N. Kosaka, T. Hiyamab and K. Nozaki, *Dalton Trans.*, 2003, 4039–4050; (*h*) T. J. Woodman, M. Schormann, D. L. Hughes and M. Bochmann, *Organometallics*, 2004, **23**, 2972–2979; (*i*) J. Cheng, D. Cui, W. Chen, N. Hu, T. Tang and B. Huang, *J. Organomet. Chem.*, 2004, **689**, 2646–2653; (*j*) H. Zhou, H. Guo, Y. Yao, L. Zhou, H. Sun, H. Sheng, Y. Zhang and Q. Shen, *Inorg. Chem.*, 2007, **46**, 958–964; (*k*) S. Zhou, S. Wang, G. Yang, Q. Li, L. Zhang, Z. Yao, Z. Zhou and H. Song, *Organometallics*, 2007, **26**, 3755–3761; (*l*) C. E. Willans, M. A. Sinenkov, G. K. Fukin, K. Sheridan, J. M. Lynam, A. A. Trifonov and F. M. Kerton, *Dalton Trans.*, 2008, 3592–3598; (*m*) M. Labet and W. Thielemans, *Chem. Soc. Rev.*, 2009, **38**, 3484–3504; (*n*) G. Du, Y. Wei, W. Zhang, Y. Dong, Z. Lin, H. He, S. Zhang and X. Li, *Dalton Trans.*, 2013, **42**, 1278–1286.

12 (*a*) S. J. Mclain and N. E. Drysdale, *Polym. Prepr.*, 1992, 174; (*b*) Z. Q. Shen, Y. Q. Shen, J. Q. Sun, F. Y. Zhang and Y. F. Zhang, *Chin. Sci. Bull.*, 1994, **39**(13), 1096; (*c*) Y. Q. Shen, Z. Q. Shen, F. Y. Zhang and Y. F. Zhang, *Polym. J.*, 1995, **27**, 59–64.

13 S. Agarwal, C. Mast, K. Dehnicke and A. Greiner, *Macromol. Rapid Commun.*, 2000, **21**, 195–212.

14 (*a*) M. Westerhausen, S. Schneiderbauer, A. N. Kneifel, Y. Söoltl, P. Mayer, H. Nöoth, Z. Zhong, P. J. Dijkstra and J. Feijen, *Eur. J. Inorg. Chem.*, 2003, 3432–3439; (*b*) M. S. Hill and P. B. Hitchcock, *Chem. Commun.*, 2003, 1758–1759; (*c*) M. H. Chisholm, J. Gallucci and K. Phomphrai, *Chem. Commun.*, 2003, 48–49; (*d*) M. H. Chisholm, J. Gallucci and K. Phomphrai, *Inorg. Chem.*, 2004, **43**, 6717–6725; (*e*) D. J. Darensbourg, W. Choi and C. P. Richers, *Macromolecules*, 2007, **40**, 3521–3523; (*f*) D. J. Darensbourg, W. Choi, O. Karroonnirun and N. Bhuvanesh, *Macromolecules*, 2008, **41**, 3493–3502; (*g*) V. Poirier, T. Roisnel, J.-F. Carpentier and Y. Sarazin, *Dalton Trans.*, 2009, 9820–9827; (*h*) X. Xu, Y. Chen, G. Zou, Z. Mac and G. Li, *J. Organomet. Chem.*, 2010, **695**, 1155–1162; (*i*) Y. Sarazin, D. Ros-ca, V. Poirier, T. Roisnel, A. Silvestru, L. Maron and J.-F. Carpentier, *Organometallics*, 2010, **29**, 6569–6577.

15 (*a*) Z. Zhong, P. J. Dijkstra, C. Birg, M. Westerhausen and J. Feijen, *Macromolecules*, 2001, **34**, 3863–3868; (*b*) D. J. Darensbourg, W. Choi, P. Ganguly and C. P. Richers, *Macromolecules*, 2006, **39**, 4374–4379; (*c*) Y. Sarazin, R. H. Howard, D. L. Hughes, S. M. Humphrey and M. Bochmann, *Dalton Trans.*, 2006, 340–350; (*d*) M. G. Davidson, C. T. O'Hara, M. D. Jones, C. G. Keir, M. F. Mahon and G. Kociok-Köohn, *Inorg. Chem.*, 2007, **46**, 7686–7688.

16 (*a*) T. P. Hanusa, *Chem. Rev.*, 1993, **93**, 1023–1036; (*b*) T. P. Hanusa, *Coord. Chem. Rev.*, 2000, **210**, 329–367; (*c*) J. S. Alexander and K. Ruhlandt-Senge, *Eur. J. Inorg. Chem.*, 2002, 2761–2774; (*d*) W. D. Buchanan, D. G. Allis and K. Ruhlandt-Senge, *Chem. Commun.*, 2010, **46**, 4449–4465.

17 M. H. Chisholm, *Inorg. Chim. Acta*, 2009, **362**, 4284–4290 and references therein.

18 (*a*) M. R. Crimmin, I. J. Casely and M. S. Hill, *J. Am. Chem. Soc.*, 2005, **127**, 2042–2043; (*b*) S. Harder and J. Brettar, *Angew. Chem., Int. Ed.*, 2006, **45**, 3474–3478; (*c*) M. R. Crimmin, M. Arrowsmith, A. G. M. Barrett, I. J. Casely, M. S. Hill and P. A. Procopiou, *J. Am. Chem. Soc.*, 2009, **131**, 9670–9685; (*d*) S. P. Sarish, S. Nembenna, S. Nagendran and H. W. Roesky, *Acc. Chem. Res.*, 2011, **44**, 157–170 and references therein.

19 (*a*) S. Datta, P. W. Roesky and S. Blechert, *Organometallics*, 2007, **26**, 4392–4394; (*b*) S. Datta, M. T. Gamer and P. W. Roesky, *Organometallics*, 2008, **27**, 1207–1213.

20 (*a*) M. Arrowsmith, M. S. Hill and G. Kociok-Köhn, *Organometallics*, 2009, **28**, 1730–1738; (*b*) M. Arrowsmith, A. Heath, M. S. Hill, P. B. Hitchcock and G. Kociok-Köhn, *Organometallics*, 2009, **28**, 4550–4559; (*c*) J. Jenter, R. Köoppe and P. W. Roesky, *Organometallics*, 2011, **30**, 1404–1413.

21 M. Arrowsmith, M. S. Hill and G. Kociok-Köhn, *Organometallics*, 2011, **30**, 1291–1294.

22 (*a*) C. Eaborn, S. A. Hawkes, P. B. Hitchcock and J. D. Smith, *Chem. Commun.*, 1997, 1961–1962; (*b*) M. J. Harvey, T. P. Hanusa and V. G. Young Jr., *Angew. Chem., Int. Ed.*, 1999, **38**, 217–219; (*c*) M. R. Crimmin, A. G. M. Barrett, M. S. Hill, D. J. MacDougall, M. F. Mahon and P. A. Procopiou, *Chem. – Eur. J.*, 2008, **14**, 11292–11295; (*d*) A. M. Johns, S. C. Chmely and T. P. Hanusa, *Inorg. Chem.*, 2009, **48**, 1380–1384; (*e*) P. Jochmann, T. S. Dols, T. P. Spaniol, L. Perrin, L. Maron and J. Okuda, *Angew. Chem., Int. Ed.*, 2009, **48**, 5715–5719; (*f*) K. Yan, B. M. Upton, A. Ellern and A. D. Sadow, *J. Am. Chem. Soc.*, 2009, **131**, 15110–15111.

23 (*a*) M. M. Gillett-Kunnath, J. G. MacLellan, C. M. Forsyth, P. C. Andrews, G. B. Deacon and K. Ruhlandt-Senge, *Chem. Commun.*, 2008, 4490–4492; (*b*) M. Göartner, H. Göorls and M. Westerhausen, *Dalton Trans.*, 2008, 1574–1582; (*c*) C. Glock, H. Göorls and M. Westerhausen, *Inorg. Chem.*, 2009, **48**, 394–399; (*d*) T. K. Panda, H. Kaneko, K. Pal, H. Tsurugi and K. Mashima, *Organometallics*, 2010, **29**, 2610–2615.

24 (*a*) M. Z. Westerhausen, *Anorg. Allg. Chem.*, 2009, **635**, 13–32; (*b*) A. G. M. Barrett, M. R. Crimmin, M. S. Hill and P. A. Procopiou, *Proc. R. Soc. London, Ser. A*, 2010, **466**, 927–963; (*c*) S. Harder, *Chem. Rev.*, 2010, **110**, 3852–3876; (*d*) S. Kobayashi and Y. Yamashita, *Acc. Chem. Res.*, 2011, **44**, 58–71.

25 K. Mashima and H. Tsurugi, *J. Organomet. Chem.*, 2005, **690**, 4414–4423 and references cited therein.

26 (*a*) L. K. Johnson, C. M. Killian and M. Brookhart, *J. Am. Chem. Soc.*, 1995, **117**, 6414–6415; (*b*) G. J. P. Britovsek, V. C. Gibson, B. S. Kimberley, P. J. Maddox, S. J. McTavish, G. A. Solan, A. J. P. White and D. J. Williams, *Chem. Commun.*, 1998, 849–850; (*c*) S. Matsui, M. Mitani, J. Saito, Y. Tohi, H. Makio, N. Matsukawa, Y. Takagi, K. Tsuru, M. Nitabaru, T. Nakano, H. Tanaka, N. Kashiwa and T. Fujita, *J. Am. Chem. Soc.*, 2001, **123**, 6847–6856 and references cited therein; (*d*) J. Tian, P. D. Hustand and G. W. Coates, *J. Am. Chem. Soc.*, 2001, **123**, 5134–5135 and references cited therein; (*e*) H. Hao, S. Bhandari, Y. Ding, H. W. Roesky, J. Magull, H. G. Schmidt, M. Noltemeyer and C. Cui, *Eur. J. Inorg. Chem.*, 2002, 1060–1065; (*f*) Y. Matsuo, K. Mashima and K. Tani, *Organometallics*, 2001, **20**, 3510–3518; (*g*) C. Cui, A. Shafir, C. L. Reeder and J. Arnold, *Organometallics*, 2003, **22**, 3357–3359.

27 T. K. Panda, K. Yamamoto, K. Yamamoto, H. Kaneko, Y. Yang, H. Tsurugi and K. Mashima, *Organometallics*, 2012, **31**, 2268–2274.

28 (*a*) R. K. Kottalanka, K. Naktode, S. Anga, H. P. Nayek and T. K. Panda, *Dalton Trans.*, 2013, **42**, 4947–4956; (*b*) R. K. Kottalanka, S. Anga, K. Naktode, P. Laskar, H. P. Nayek and T. K. Panda, *Organometallics*, 2013, **32**, 4473–4482; (*c*) R. K. Kottalanka, P. Laskar, K. Naktode, B. S. Mallik and T. K. Panda, *J. Mol. Struct.*, 2013, **1047**, 302–309; (*d*) R. K. Kottalanka, A. Harinath, J. Bhattacharjee, H. V. Babu and T. K. Panda, *Dalton Trans.*, 2014, 8757–8766; (*e*) J. Bhattacharjee, R. K. Kottalanka, A. Harinath and T. K. Panda, *J. Chem. Sci.*, 2014, **126**, 1463–1475; (*f*) R. K. Kottalanka, A. Harinath and T. K. Panda, *RSC Adv.*, 2015, **5**, 37755–37767.

29 Y. Yang, Bo. Liu, K. Lv, W. Gao, D. Cui, X. Chen and X. Jing, *Organometallics*, 2007, **26**, 4575–4584.

30 Y. Yang, S. Li, D. Cui, X. Chen and X. Jing, *Organometallics*, 2007, **26**, 671–678.

31 S. B. Clara, D. Gomes, P. T. Suresh, L. F. Gomes, M. T. Veiros, G. N. Teresa and M. C. Oliveira, *Dalton Trans.*, 2010, **39**, 736–748.

32 S. A. Carabineiro, L. C. Silva, P. T. Gomes, L. C. J. Pereira, L. F. Veiros, S. I. Pascu, M. T. Duarte, S. Namorado and R. T. Henriques, *Inorg. Chem.*, 2007, **46**, 6880–6890.

33 The bonding situation in the drawing of the ligand system is simplified for clarity.

34 Q. Li, J. Rong, S. Wang, S. Zhou, L. Zhang, X. Zhu, F. Wang, S. Yang and Y. Wei, *Organometallics*, 2011, **30**, 992–1001.

35 (*a*) W. T. Klooster, L. Brammer, C. J. Schaverien and P. H. M. Budzelaar, *J. Am. Chem. Soc.*, 1999, **121**, 1381–1382; (*b*) W. Scherer and G. S. McGrady, *Angew. Chem., Int. Ed.*, 2004, **43**, 1782–1806.

36 (*a*) S. De Angelis, E. Solan, C. Flonani, A. Chiesi-Villa and C. Rizzoli, *J. Am. Chem. Soc.*, 1994, **116**, 5702–5713; (*b*) S. De Angelis, E. Solari, C. Floriani, A. Chiesi-Villa and C. Rizzoli, *J. Chem. Soc., Dalton Trans.*, 1994, 2467–2469; (*c*) J. Jubb, S. Gambarotta, R. Duchateau and J. H. Teuben, *J. Chem. Soc., Chem. Commun.*, 1994, 2641–2642; (*d*) D. Jacoby, S. Isoz, C. Floriani, A. Chiesi-Villa and C. Rizzoli, *J. Am. Chem. Soc.*, 1995, **117**, 2805–2816; (*e*) L. Bonomo, E. Solari, R. Scopelliti, C. Floriani and N. Re, *J. Am. Chem. Soc.*, 2000, **122**, 5312–5326.

37 J. Gao, Y. Liu, Y. Zhao, X.-J. Yang and Y. Sui, *Organometallics*, 2011, **30**, 6071–6077.

38 L.-F. Hsueh, N.-T. Chuang, C.-Y. Lee, A. Datta, J.-H. Huang and T.-Y. Lee, *Eur. J. Inorg. Chem.*, 2011, 5530–5537.

39 G. J. Moxey, F. Ortu, L. G. Sidley, H. N. Strandberg, A. J. Blake, W. Lewis and D. L. Kays, *Dalton Trans.*, 2014, **43**, 4838–4846.

40 P. J. Bailey, R. A. Coxall, C. M. Dick, S. Fabre, L. C. Henderson, C. Herber, S. T. Liddle, D. Loroño-Gonzalez, A. Parkin and S. Parsons, *Chem. – Eur. J.*, 2003, **9**, 4820–4828.

41 (*a*) S. Harder, S. Müller and E. Hübner, *Organometallics*, 2004, **23**, 178–183; (*b*) O. Michel, C. Meermann, K. W. Toürnroos and R. Anwander, *Organometallics*, 2009, **28**, 4783–4790.

42 T. K. Panda, H. Kaneko, O. Michel, H. Tsurugi, K. Pal, K. W. Toernroos, R. Anwander and K. Mashima, *Organometallics*, 2012, **31**, 3178–3184.

43 (*a*) L. F. Sánchez-Barba, D. L. Hughes, S. M. Humphrey and M. Bochmann, *Organometallics*, 2006, **25**, 1012–1020; (*b*) L. F. Sánchez-Barba, D. L. Hughes, S. M. Humphrey and M. Bochmann, *Organometallics*, 2005, **24**, 5329–5334; (*c*) L. F. Sánchez-Barba, D. L. Hughes, S. M. Humphrey and M. Bochmann, *Organometallics*, 2005, **24**, 3792–3799.

44 A. Garcés, L. F. Sánchez-Barba, C. Alonso-Moreno, M. Fajardo, J. Fernández-Baeza, A. Otero, A. Lara-Sánchez, I. López-Solera and A. M. Rodríguez, *Inorg. Chem.*, 2010, **49**, 2859–2871.

45 M. Kuzdrowska, L. Annunziata, S. Marks, M. Schmid, C. G. Jaffredo, P. W. Roesky, S. M. Guillaume and L. Maron, *Dalton Trans.*, 2013, **42**, 9352–9360.

46 M. G. Cushion and P. Mountford, *Chem. Commun.*, 2011, **47**, 2276–2278.

47 B. Liu, T. Roisnel, J.-P. Guegan, J.-F. Carpentier and Y. Sarazin, *Chem. – Eur. J.*, 2012, **18**, 6289–6301.

48 Y. Sarazin, B. Liu, L. Maron and J.-F. Carpentier, *J. Am. Chem. Soc.*, 2011, **133**, 9069–9087.

49 M. Westerhausen, *Coord. Chem. Rev.*, 1998, **176**, 157–210.

50 D. George, K. Vaughn, K. Alex and J. A. Gladysz, *Organometallics*, 1986, **5**, 936–942.

51 A. Altomare, M. C. Burla, G. Camalli, G. Cascarano, C. Giacovazzo, A. Gualiardi and G. Polidori, *J. Appl. Crystallogr.*, 1994, **27**, 435.

52 G. M. Sheldrick, *Acta Crystallogr., Sect. A: Fundam. Crystallogr.*, 2008, **64**, 112.